Synthesis of Dinuclear Anionic Complexes $[Cp^*Rh(CO)]_2^-$ and $[Cp^*Rh(CO)]_2^{2-}$ by Dissolving Metal Reduction and $R[Cp^*Rh(CO)]_2^-$ by Addition of Alkyllithium Reagents across the Metal–Metal Double Bond of $[Cp^*Rh(CO)]_2$. Stereoselective Synthesis of Symmetrical and Mixed Dinuclear Dialkyls $[Cp^*{}_2Rh_2(CO)_2(R_1)(R_2)]$ and a Study of Their Ligand-Induced Fragmentation Reactions

Michael J. Krause and Robert G. Bergman*

Department of Chemistry, University of California, Berkeley, California 94720

Received February 10, 1986

Chemical reduction of $[Cp^*RhCO]_2$ ($Cp^* = \eta^5\text{-}C_5Me_5$) leads initially to $[Cp^*RhCO]_2^-$, isolated as the K^+ or K(cryptate)$^+$ salts. This 33-valence-electron radical anion was further reduced to give the unusual dianion $[Cp^*RhCO]_2^{2-}$, isolated as both the $(K^+)_2$ and the $[K(cryptate)^+]_2$ salts. Both radical anion and dianion were alkylated in low yield to give dinuclear dialkyl compounds $[Cp^*Rh(CO)R]_2$. The potassium salt of the dianion was characterized by a single-crystal X-ray diffraction study; the crystal structure showed an arrangement in which two dimeric dianions are coordinated to an approximate square of potassium cations. Crystal data on $K_2Rh_2(\mu\text{-}CO)_2(C_5(CH_3)_5)_2\cdot(C_4H_8O)_2$: triclinic, $P\bar{1}$, $a = 12.1653$ (13) Å, $b = 15.2618$ (24) Å, $c = 19.2691$ (28) Å, $\alpha = 84.424$ (12)°, $\beta = 87.851$ (11)°, $\gamma = 77.837$ (11)°, $V = 3479.9$ (12) Å^3, $Z = 4$; Mo Kα radiation, $\lambda = 0.710\,73$ Å; 9065 reflections, 6011 $F^2 > 3\sigma(F^2)$; corrected for decay, empirically corrected for absorption; $R = 4.75\%$, $wR = 7.66\%$. A more satisfactory synthesis of these materials was achieved by the first example of addition of alkyllithium reagents across the metal–metal multiple bond of $[Cp^*RhCO]_2$. In this way methyl-, phenyl-, and ethyllithium led to solutions of adducts proposed to be $Li[Cp^*{}_2Rh_2(CO)_2(R)]$, containing a negatively charged rhodium atom and a new metal–carbon bond. Treatment of these solutions with primary alkyl *p*-toluenesulfonates gives good yields of both symmetrical and unsymmetrical dinuclear dialkyl complexes $Cp^*{}_2Rh_2(CO)_2(R_1)(R_2)$. The symmetrical complexes ($R_1 = R_2$) were identical with those formed as mixtures from $[Cp^*RhCO]_2^-$ and $[Cp^*RhCO]_2^{2-}$. Only one stereoisomer of the dialkyl complexes, presumed to be the cis, is formed as kinetic product of these reactions; isomerization of the cis complexes to their trans isomers occurs slowly in solution. Treatment of the dimethyl complex $[Cp^*Rh(CO)(CH_3)]_2$ with dative ligands causes clean fragmentation. CO gives $Cp^*Rh(CO)_2$ and $Cp^*RhCO(CH_3)_2$; surprisingly, PPh_3 leads to $Cp^*Rh(CO)_2$ and $Cp^*Rh(PPh_3)(CH_3)_2$. Preliminary kinetic studies demonstrate that the rate of the latter reaction does not depend on the concentration of phosphine, and thus rate-determining formation of a transient intermediate (proposed to have a methyl group bridging the two metal centers) is involved in the process.

Introduction

A wide variety of polynuclear complexes, either metal clusters[1] or compounds with multiple metal–metal bonds,[2] have been synthesized. Studies on these compounds have been limited largely to determining the nature of the metal–metal bond,[2] exploring the unusual structural features of organic groups connected to more than one metal atom,[3] or observing the stoichiometric or catalytic reactions of polynuclear complexes with various substrates.[2,3c,4]

Mechanistically, polynuclear complexes can potentially generate unique reactivity by the cooperative interaction of two or more metal centers. Alternatively, they may react similarly to their mononuclear counterparts, especially in cases where reactions take place at only one metal center, or cleavage into reactive mononuclear fragments occurs. Relatively few detailed mechanistic studies have been carried out to examine these choices. Understandably, those which are known have so far focused mainly on dinuclear complexes.[5-10]

Scheme I

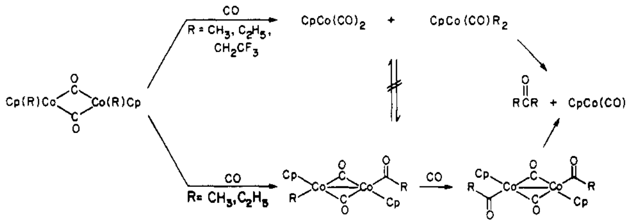

---

[1] (a) Vahrenkamp, H. *Adv. Organomet. Chem.* **1983**, *22*, 169. (b) Muetterties, E. L. *J. Organomet. Chem.* **1980**, *200*, 177. (c) Chini, P. *J. Organomet. Chem.* **1980**, *200*, 37. (d) King, R. B. *Progr. Inorg. Chem.* **1972**, *15*, 287. (e) Corbett, J. D. *Progr. Inorg. Chem.* **1976**, *21*, 129. (f) Chini, P.; Longoni, G.; Albano, V. C. *Adv. Organomet. Chem.* **1976**, *14*, 285.

[2] Cotton, F. A.; Walton, R. A. *Multiple Bonds between Metal Atoms*; Wiley: New York, 1982.

[3] (a) Herrmann, W. A. *Adv. Organomet. Chem.* **1982**, *20*, 160. (b) Herrmann, W. A. *J. Organomet. Chem.* **1983**, *250*, 319. (c) Muetterties, E. L.; Rhodin, T. N.; Band, E.; Brucker, C. F.; Pretzer, W. R. *Chem. Rev.* **1979**, *79*, 91 and references therein. (d) Tachikawa, M.; Muetterties, E. L. *Prog. Inorg. Chem.* **1981**, *28*, 203.

[4] (a) Muetterties, E. L.; Stein, J. Chem. Rev. **1979**, *79*, 479. (b) Muetterties, E. L.; Krause, M. J. *Angew. Chem., Int. Ed. Engl.* **1983**, *22*, 135 and references therein. (c) Chisolm, M. H. *ACS Symp. Ser.* **1981**, *No. 155*, 17. (d) Muetterties, E. L.; Burch, R. R.; Stolzenberg, A. M. *Annu. Rev. Phys. Chem.* **1982**, *33*, 89.

[5] See for example, (a) Knox, S. A. R.; Stansfield, R. F. D.; Stone, F. G. A.; Winter, M. J.; Woodward, P. *J. Chem. Soc., Dalton Trans.* **1982**, 173. (b) Sonnenberger, D.; Atwood, J. D. *J. Am. Chem. Soc.* **1980**, *102*, 3484. (c) Amer, S.; Poe, A. *J. Organomet. Chem.* **1981**, *209*, C31. (d) Forbus, N. P.; Oteiza, R.; Smith, S. G.; Brown, T. L. *J. Organomet. Chem.* **1980**, *193*, C71. (e) Steigman, A. E.; Tyler, D. R. *J. Am. Chem. Soc.* **1982**, *104*, 2944. (f) Schmidt, S. P.; Trogler, W. C.; Basolo, F. *J. Am. Chem. Soc.* **1982**, *21*, 1699. (g) Poe, A.; Marcomini, A. *J. Chem. Soc., Dalton Trans.* **1984**, 95. (h) Tyler, D. R.; Schmidt, M. A.; Gray, H. B. *J. Am. Chem. Soc.* **1983**, *105*, 6018. (i) Azam, K. A.; Puddephatt, R. J. *Organometallics* **1983**, 2, 1396. (j) Stiegman, A. E.; Tyler, D. R. *Acc. Chem. Res.* **1984**, *17*, 61. (k) Lee, K.-W.; Pennington, W. T.; Cordes, A. W.; Brown, T. L. *J. Am. Chem. Soc.* **1985**, *107*, 631. (l) Sundarajan, G.; San Filippo, J. *Organometallics* **1985**, *4*, 606. (m) Anderson, L. B.; Cotton, F. A.; DeMarco, D.; Falvello, L. R.; Tetrick, S. M.; Walton, R. A. *J. Am. Chem. Soc.* **1984**, *106*, 4743. (n) Schmidt, S. P.; Trogler, W. C.; Basolo, F. *J. Am. Chem. Soc.* **1984**, *103* 1308.

0276-7333/86/2305-2097$01.50/0

Scheme II

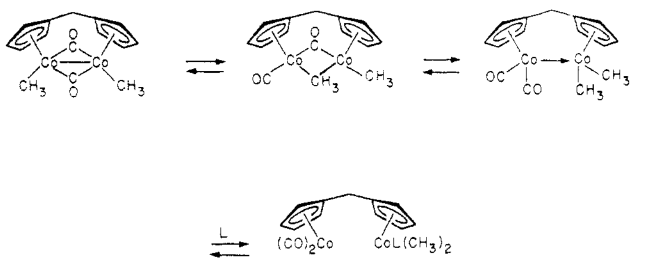

Our own interest in the mechanisms of reaction of dinuclear complexes has focused on systems containing one or more alkyl groups, where the possibility exists for dimetal-mediated formation of new carbon–carbon bonds. This work began with the discovery that dissolving metal reduction of $CpCo(CO)_2$ leads to salts of $[CpCo(CO)]_2^-$, a 33-valence-electron dinuclear radical anion,[6] and the finding that this material could be converted to a wide range of dinuclear dialkyl and metallacycle complexes.[6-10] A related dimethyl complex with the two Cp ligands linked together by a methylene bridge has also been prepared.[10b]

The dialkyl complexes and metallacycles undergo a series of apparent CO insertion and/or reductive elimination reactions. The mechanisms of these processes have been studied in some detail. In the case of the dialkyl complexes, thermal decomposition leads to ketones R–CO–R, $CpCo(CO)_2$, and cobalt cluster complexes. Carbonylation of the dialkyls leads to nearly quantitative formation of ketones and $CpCo(CO)_2$. When R = CH_3 or C_2H_5, the mechanism of this carbonylation proceeds through two independent pathways, as shown in Scheme I. One involves initial fragmentation to form $CpCo(CO)_2$ and $CpCo(CO)R_2$; mononuclear insertion/reductive elimination then occurs in the latter complex to give ketone. The second pathway involves initial carbonylation to give dinuclear acyl and diacyl complexes, which serve as intermediates in a more rapid route to ketones.[9-11]

Linking the two Cp rings together with a methylene bridge alters the chemical and mechanistic behavior of these systems, as shown in Scheme II. Carbonylation of the linked-ring dimethyl complex $[(C_5H_4)CH_2(C_5H_4)]$-$[Co(CH_3)(CO)]_2$ gives acetone and the dinuclear carbonyl complex $[C_5H_4)CH_2(C_5H_4)][Co_2(CO)_4$. Here, however, no dinuclear diacyl complexes are detected. Most surprisingly, a clean, rapid reaction occurs with PPh_3, which leads *reversibly* to the dinuclear complex $(CO)_2Co(C_5H_4)CH_2$-$(C_5H_4)Co(PPh_3)(CH_3)_2$. The mechanism summarized in Scheme II has been proposed for this process.[10b]

Although much has been learned about the mechanisms of these reactions, information normally accessible from certain critical labeling experiments, such as crossover experiments, has been difficult to gather due to the fact that the dialkyl complexes $[CpCo(CO)(R)]_2$ undergo very rapid, reversible fragmentation in solution into 17-electron CpCo(CO)R monomers. It is not yet completely clear whether these monomers, which are present in the low concentration but are very reactive, are involved in either or both of the mechanistic pathways summarized above. In addition, the clean and somewhat surprising reaction of the linked-ring system with PPh_3 could not be investigated in the parent system; complicated product mixtures were obtained on treatment of $[CpCo(CO)(R)]_2$ with phosphines.

We have tried for some time to extend this chemistry into the rhodium system, in hopes of obtaining products with stronger metal–metal bonds to prevent the fragmentation into 17-electron monomers. Unfortunately, reduction of $CpRh(CO)_2$ does not give $[CpRh(CO)]_2^-$, the radical anion analogous to that formed from the cobalt complex, but instead leads[11] to the trinuclear anion $[Cp_2Rh_3(CO)_4]^-$. Therefore, a more direct route to a rhodium radical anion was needed. $[Cp^*RhCO]_2$ (Cp^* = η^5-$C_5(CH_3)_5$), a 32-valence-electron complex with a formal metal-metal double bond, has been known since 1979[12] and has been used as a precursor to a large variety of organometallic and inorganic species.[13-28] In this paper we report:

---

(6) (a) Ilenda, C. S.; Schore, N. E.; Bergman, R. G. *J. Am. Chem. Soc.* **1976**, *98*, 255. (b) Schore, N. E.; Ilenda, C. S.; Bergman, R. G. *J. Am. Chem. Soc.* **1976**, *98*, 256. (c) Schore, N. E.; Ilenda, C. S.; Bergman, R. G. *J. Am. Chem. Soc.* **1977**, *99*, 1781.

(7) (a) Schore, N. E.; Ilenda, C.; Bergman, R. G. *J. Am. Chem. Soc.* **1976**, *98*, 7436. (b) Schore, N. E.; Ilenda, C. S.; White, M. A.; Bryndza, H. E.; Matturro, M. G.; Bergman, R. G. *J. Am. Chem. Soc.* **1984**, *106*, 7451. (c) $[Cp^*Co(CO)(CH_3)]$ is prepared by an alternate route: Bunel, E. E.; Valle, L.; Manriquez, J. M. *Organometallics* **1985**, *4*, 1680.

(8) (a) Theopold, K. H.; Bergman, R. G. *J. Am. Chem. Soc.* **1980**, *102*, 5694. (b) Theopold, K. H.; Bergman, R. G. *J. Am. Chem. Soc.* **1981**, *1034*, 2489. (c) Theopold, K. H.; Hersh, W. H.; Bergman, R. G. *Isr. J. Chem.* **1982**, *102*, 27. (d) Hersh, W. H.; Bergman, R. G. *J. Am. Chem. Soc.* **1981**, *103*, 6992. (e) Theopold, K. H.; Bergman, R. G. *Organometallics* **1982**, *1*, 219. (f) Theopold, K. H.; Bergman, R. G. *J. Am. Chem. Soc.* **1983**, *105*, 464. (g) Theopold, K. H.; Bergman, R. G. *Organometallics*, **1982**, *1*, 1571. (h) Hersh, W. H.; Hollander, F. J.; Bergman, R. G. *J. Am. Chem. Soc.* **1983**, *105*, 5834. (i) Hersh, W. H.; Bergman, R. G. *J. Am. Chem. Soc.* **1983**, *105*, 5846.

(9) (a) Jacobsen, E. N.; Bergman, R. G. *Organometallics* **1984**, *3*, 329. (b) Jacobsen, E. N.; Bergman, R. G. *J. Am. Chem. Soc.* **1985**, *107*, 2023.

(10) (a) Bergman, R. G. *Acc. Chem. Res.* **1980**, *13*, 113. (b) Bryndza, H. E.; Bergman, R. G. *J. Am. Chem. Soc.* **1979**, *101*, 4766. (c) White, M. A.; Bergman, R. G. *J. Am. Chem., Chem. Commun.* **1979**, 1056. (d) Theopold, K. H.; Becker, P. N.; Bergman, R. G. *J. Am. Chem. Soc.* **1982**, *104*, 5250. (e) Yang, G. K.; Bergman, R. G. *J. Am. Chem. Soc.* **1983**, *105*, 6045.

(11) Jones, W. D.; White, M. A.; Bergman, R. G. *J. Am. Chem. Soc.* **1978**, *100*, 6770.

(12) Nutton, A.; Maitlis, P. M. *J. Organomet. Chem.* **1979**, *166*, C21.

(13) (a) Aldridge, M. L.; Green, M.; Howard, J. A. K.; Pain, G. N.; Porter, S. J.; Stone, F. G. A.; Woodward, P. *J. Chem. Soc., Dalton Trans.* **1982**, 1333. (b) Herrmann, W. A.; Plank, J.; Bauer, C.; Ziegler, M. L.; Guggolz, E.; Alt, R. *Z. Anorg. Allg. Chem.* **1982**, *487*, 85.

(14) Green, M.; Hankey, D. R.; Howard, J. A. K.; Louca, P.; Stone, F. G. A. *J. Chem. Soc., Chem. Commun.* **1983**, 757.

(15) (a) Boag, N. M.; Green, M.; Mills, R. M.; Pain, G. N.; Stone, F. G. A.; Woodward, P. *J. Chem. Soc., Chem. Commun.* **1980**, 1171. (b) Green, M.; Howard, J. A. K.; Mills, R. M.; Pain, G. N.; Stone, F. G. A.; Woodward, P. *J. Chem. Soc., Chem. Commun.* **1981**, 869. (c) Green, M.; Howard, J. A. K.; Pain, G. N.; Stone, F. G. A. *J. Chem. Soc., Dalton Trans.* **1982**, 1327. (d) Bray, A. C.; Green, M.; Hankey, D. R.; Howard, J. A. K.; Johnson, O.; Stone, F. G. A. *J. Organomet. Chem.* **1985**, *281*, C12.

(16) (a) Carriedo, G. A.; Howard, J. A. K.; Stone, F. G. A. *J. Organomet. Chem.* **1983**, *250*, C28. (b) Carriedo; G. A.; Howard, J. A. K.; Stone, F. G. A. *J. Chem. Soc., Dalton Trans.* **1984**, 1555;

(17) (a) Herrmann, W. A.; Bauer, C.; Weichmann, J. *J. Organomet. Chem.* **1983**, *243*, C21. (b) Herrmann, W. A.; Bauer, C.; Weichmann, J. *Chem. Ber.* **1984**, *117*, 1271.

(18) Barr, R. D.; Green, M.; Marsden, K.; Stone, F. G. A.; Woodward, P. *J. Chem. Soc., Dalton Trans.* **1983**, 507.

(19) (a) Barr, R. D.; Green, M.; Howard, J. A. K.; Marder, T. B.; Stone, F. G. A. *J. Chem. Soc., Chem. Commun.* **1983**, 759. (b) Barr, R. D.; Green, M.; Howard, J. A. K.; Marder, T. B.; Orpen, A. G.; Stone, F. G. A. *J. Chem. Soc., Dalton Trans.* **1984**, 2757.

(20) (a) Chetcuti, M.; Green, M.; Howard, J. A. K.; Jeffery, J. C.; Mills, R. M.; Pain, G. N.; Porter, S. J.; Stone, F. G. A.; Wilson, A. A.; Woodward, P. *J. Chem. Soc., Chem. Commun.* **1980**, 1057. (b) Green, M.; Jeffery, J. C.; Porter, S. J.; Razay, H.; Stone, F. G. A. *J. Chem. Soc., Dalton Trans.* **1982**, 2475. (c) Jeffery, J. C.; Marsden, C.; Stone, F. G. A. *J. Chem. Soc., Dalton Trans.* **1985**, 1315.

(21) Farrugia, L. J.; Orpen, A. G.; Stone, F. G. A. *Polyhedron* **1983**, *2*, 171.

(22) (a) Green, M.; Mills, R. M.; Pain, G. N.; Stone, F. G. A.; Woodward, P. *J. Chem. Soc., Dalton Trans.* **1982**, 1309. (b) Clauss, A. D.; Dimas, P. A.; Shapley, J. R. *J. Organomet. Chem.* **1980**, *201*, C31. (c) Herrmann, W. A.; Bauer, C.; Kriechbaum, G.; Kunkely, H.; Ziegler, M. L.; Speth, D.; Guggolz, E. *Chem. Ber.* **1982**, *115*, 878.

(1) the one- and the unique two-electron reduction of this material and alkylation of the reduced species to form new rhodium dialkyl complexes and dimetallacycles, (2) stepwise dialkylation of $[Cp^*RhCO]_2$ by initial addition of a formal R^- source followed by addition of a formal R^+ source, and (3) some of the reaction chemistry of $[Cp^*Rh(CO)(CH_3)]_2$ including a kinetic study of its reaction with $P(C_6H_5)_3$.

Experimental Section

General Data. All reductions were performed in an "H-tube" reactor[29] under static high vacuum conditions (10^{-5} torr). All other manipulations were performed by using standard Schlenk techniques under argon or in a Vacuum Atmospheres inert-atmospheres box under N_2 or Ar, prescrubbed and continuously circulated through a purifier. All organometallic anions described were extremely air- and moisture-sensitive; the organometallic dialkyl and dimetallacycle compounds were slightly air-sensitive. Sodium balls and potassium sticks in mineral oil were purchased from Aldrich; the mineral oil was removed by washing with hexanes immediately before use. Sodium/potassium alloy was 70% by weight potassium. Alumina was purchased from Alfa and deactivated with 6% H_2O by weight: Florisil was purchased from Fisher Scientific and used as received. All solvents and liquid reagents were degassed by several freeze–evacuate–thaw cycles. THF and THF-d_8 were dried over Na–benzophenone ketyl. Pentane, toluene, hexamethyldisiloxane, C_6D_6, and toluene-d_8 were dried over Na/K–benzophenone ketyl; a small amount of triglyme was added to the pentane and toluene to solubilize the ketyl. CH_2Cl_2 and CH_3I were dried over Na/Pb alloy (Fluka). CD_3I was dried over 3Å molecular sieves and stored in the dark over copper wire. $RhCl_3{\cdot}3H_2O$ was purchased from Johnson-Matthey and used as received. $C_5(CH_3)_5H$ was purchased from Strem and used as received or was prepared by the literature procedure.[30] $[Cp^*RhCO]_2$ was prepared by literature methods.[13] Kryptofix 2,2,2 (4,7,13,16,21,24-hexaoxa-1,10-diazabicyclo[8.8.8]hexacosane) was purchased from Fluka and used as received. Methyl *p*-toluenesulfonate (MeOTs) and ethyl *p*-toluenesulfonate (EtOTs) were purchased from Aldrich and used as received. $(TsO)(CH_2)_3(OTs)$ was the gift of Dr. Gilbert Yang. Methyllithium was purchased as a 1.6 M diethyl ether solution from Fluka and used as received. Ethyllithium was the gift of Dr. Roy Periana. Carbon monoxide, ethylene, and acetylene were obtained from the Lawrence Berkeley Laboratory and used as received. Trimethylphosphine was purchased from Strem and dried over Na/K. Triphenylphosphine was purchased from Aldrich and recrystallized before use.

NMR, mass, and IR spectra were recorded, and data are reported, by using conventional procedures. Magnetic susceptibility was measured by using a S.H.E. Corp. superconducting magnetometer (SQUID) at 5 and 40 kG over the temperature range 6–280 K. Microanalyses were performed by the UC Berkeley microanalytical laboratory.

$K^+[Cp^*RhCO]_2^-$. Approximately 10 mL of THF was vacuum distilled onto 50 mg (0.094 mmol) of $[Cp^*RhCO]_2$ and 10 mg of Na/K alloy. The resulting solution was stirred until the color changed from navy blue to translucent forest green (approximately 0.5–1.5 h). This solution was filtered, and the solvent volume was reduced under vacuum to approximately 3 mL. The solution was cooled to −78 °C, and ca. 10 mL pentane was vacuum distilled on top of the THF layer. The solvent layers were allowed to mix by diffusion at room temperature. Removal of solvent by filtration and drying in high vacuum led to the isolation of 8 mg (0.014 mmol, 15%) of $K^+[Cp^*RhCO]_2^-$ as green-black feathery needles. ESR (THF): broad singlet, $g = 2.08$. IR (THF): 1631 (s, br), 1670 (m, br) cm^{-1} (decomposition peak due to $[Cp^*RhCO_2]$ observed at 1736 cm^{-1}). IR (Nujol mull): 1675 (v br) cm^{-1} (decomposition peak due to $[Cp^*RhCO]_2$ observed at 1730 cm^{-1}). Anal. Calcd for $C_{22}H_{30}O_2Rh_2K$: C, 46.25; H, 5.29; K, 6.74. Found: C, 45.97; H, 5.41; K, 6.78.

$[K(crypt)^+][Cp^*RhCO]_2^-$. A solution of $K^+[Cp^*RhCO]_2^-$ was generated as described above. This was filtered onto 35 mg (0.093 mmol) of Kryptofix 2,2,2 and the resulting solution stirred for 0.5 h. This solution was reduced in volume to approximately 5 mL and cooled to −78 °C, and ca. 10 mL of was pentane vacuum distilled on top. Slow diffusion of the solvents at room temperature, followed by filtration and drying under high vacuum, left dark green, feathery needles of $[K(crypt)^+][Cp^*RhCO]_2^-$ (28 mg, 0.30 mmol, 31%). ESR (2-methyltetrahydrofuran): broad singlet ($\omega_{1/2} = 28$ G), $g = 2.070$. IR (THF): 1670 cm^{-1} (decomposition peak due to $[Cp^*RhCO]_2$ observed at 1736 cm^{-1}). IR (Nujol mull): 1664 cm^{-1} (decomposition peak due to $[Cp^*RhCO]_2$ observed at 1730 cm^{-1}). UV max (THF): 353 (ϵ 2.5 × 10^4), 472 (6.9 × 10^3), 586 (5.9 × 10^3) nm. Magnetic susceptibility (Curie–Weiss behavior; corrected for sample and container diamagnetism): at 5 kG, $C = 0.415$ (1), $\theta = -1.26 \pm 0.14$ K, $\mu_{eff} = 1.823$ (2) μ_B; at 40 kG, $C = 0.416$ (1), $\theta = -1.05 \pm 0.25$ K, $\mu_{eff} = 1.823$ (4) μ_B. Anal. Calcd for $C_{40}H_{66}N_2O_8Rh_2K$: C, 50.69; H, 7.02; N, 2.96; K, 4.13. Found: C, 50.43; H, 6.97; N, 2.77; K, 4.10.

$(K^+)_2[Cp^*RhCO]_2^{2-}$. Approximately 10 mL of THF was vacuum distilled onto 50 mg (0.094 mmol) of $[Cp^*RhCO]_2$ and 15 mg of Na/K alloy. The resulting solution was stirred at room temperature until the color changed from navy blue to forest-green and then to translucent dark red (approximately 1–2 h). The solution was filtered and reduced in volume to approximately 3 mL. This solution was cooled to −78 °C, and ca. 10 mL of pentane was vacuum distilled to form a layer on top. Slow diffusion of the solvents at room temperature led to dark red crystals of $(K^+)_2[Cp^*RhCO]_2^{2-}$ which was isolated by filtration and dried under high vacuum (30 mg, 0.049 mmol, 52%). ^1H NMR (THF-d_8): δ1.92 (s). IR (THF): 1747, 1690, 1669, 1635, 1588 cm^{-1}. Anal. Calcd for $C_{22}H_{30}O_2Rh_2K_2$: C, 43.28; H, 4.95; K, 12.8. Found: C, 43.19; H, 5.09; K, 12.1.

$[K(crypt)^+]_2[Cp^*RhCO]_2^{2-}$. A solution of $(K^+)_2[Cp^*RhCO]_2^{2-}$ was generated as described above. This was filtered onto 70 mg (0.19 mmol) of 2,2,2 Kryptofix, and the resulting solution was stirred for 0.5–1 h. The solution was reduced in volume to approximately 5 mL and was cooled to −78 °C, and ca. 10 mL of pentane was vacuum distilled on top. Slow diffusion of the solvent layers at room temperature, followed by filtration and drying under high vacuum left 35 mg (0.025 mmol, 27%) of $[K(crypt)^+]_2[Cp^*RhCO]_2^{2-}$ as a dark red powder. ^1H NMR (THF-d_8): δ 3.55 (br s), 3.52 (br s), 2.54 (br s), 1.92 (s). IR (THF): 1743 (br, w), 1694 (m), 1669 (s) cm^{-1}. Anal. Calcd for $C_{58}H_{102}N_4O_{14}Rh_2K_2$: C, 51.09; H, 7.54; N, 4.11; K, 5.74. Found: C, 51.49; H, 7.76; N, 3.55; K, 5.29.

$[Cp^*RhCO]_2(\mu\text{-}CH_2)$. A solution of $(K^+)_2[Cp^*RhCO]_2^{2-}$ was generated from 50 mg (0.094 mmol) of $[Cp^*RhCO]_2$ as described

---

(23) (a) Bauer, C.; Guggolz, E.; Herrmann, W. A.; Kriechbaum, G.; Ziegler, M. L. *Angew. Chem., Int. Ed. Engl.* **1982**, *21*, 212. (b) Bauer, C.; Herrmann, W. A. *J. Organomet. Chem.* **1981**, *209*, C13. (c) Herrmann, W. A.; Bauer, C.; Mayer, K. K. *J. Organomet. Chem.* **1982**, *236*, C18. (d) Herrmann, W. A.; Kriechbaum, G. W.; Bauer, C.; Koumbouris, B.; Pfisterer, H.; Guggolz, E.; Ziegler, M. L. *J. Organomet. Chem.* **1984**, *262*, 89. (e) Herrmann, W. A.; Weber, C. *J. Organomet. Chem.* **1985**, *282*, C31. (f) Herrmann, W. A.; Huggins, J. M. *Chem. Ber.* **1982**, *115*, 396. (g) Herrmann, W. A.; Bauer, C.; Kriechbaum, G.; Kunkely, H.; Ziegler, M. L.; Speth, D.; Guggolz, E. *Chem. Ber.* **1982**, *115*, 878. (h) Herrmann, W. A.; Weber, C.; Ziegler, M. L.; Pahl; C. *Chem. Ber.* **1984**, *117*, 875. (i) Herrmann, W. A.; Plank, J.; Hubbard, J. L.; Kriechbaum, G. W.; Kalcher, W.; Koumbouris, B.; Ihl, G.; Schafer, A.; Ziegler, M. L.; Pfisterer, H.; Pahl, C.; Atwood, J. L.; Rogers, R. D. *Z. Naturforsch., B.: Anorg. Chem., Org. Chem.* **1983**, *388*, 1392. (j) Herrmann, W. A.; Bauer, C.; Ziegler, M. L.; Pfisterer, H. *J. Organomet. Chem.* **1983**, *243*, C54.

(24) Herrmann, W. A.; Plank, J.; Riedel, D.; Ziegler, M. L.; Weidenhammer K.; Guggolz, E.; Balbach, B. *J. Am. Chem. Soc.* **1981**, *103*, 63.

(25) (a) Werner, H.; Klingert, B. *J. Organomet. Chem.* **1982**, *233*, 365. (b) Werner, H.; Klingert, B.; Zolk, R.; Thometzek, P. *J. Organomet. Chem.* **1984**, *266*, 97.

(26) Schaverien, C. J.; Green, M.; Orpen, A. G.; Williams, I. D. *J. Chem. Soc., Chem. Commun.* **1982**, 912.

(27) (a) Dickson, R. S.; Evans, G. S.; Fallon, G. D. *J. Organomet. Chem.* **1982**, *236*, C49. (b) Herrmann, W. A.; Bauer, C.; Schafer, A. *J. Organomet. Chem.* **1983**, *256*, 147. (c) Dickson, R. S.; Evans, G. S.; Fallon, G. D. *Aust. J. Chem.* **1985**, *38*, 273. (d) Becker, G.; Herrmann, W. A.; Kalcher, W.; Kriechbaum, G. W.; Pahl, C.; Wagner, C. T.; Ziegler, M. L. *Angew. Chem., Int. Ed. Engl.* **1983**, *22*, 413.

(28) Part of the work described here was reported earlier in preliminary form: Krause, M. J.; Bergman, R. G. *J. Am. Chem. Soc.* **1985**, *107*, 2972.

(29) An "H-tube" is an all glass reactor that contains two chambers connected by a glass frit. The two chambers are topped by ground glass joints which permit easy filling and emptying of the ports as well as a way to connect the apparatus to the vacuum line. Kulzick, M. A. Ph.D. dissertation, University of California, Berkeley, CA, 1984.

(30) Threlkel, R. S.; Bercaw, J. E. *J. Organomet. Chem.* **1977**, *136*, 1.

above. This red solution was filtered; subsequent addition of ca. 0.5 mL of CH_2Cl_2 by vacuum transfer at room temperature immediately caused the solution color to change to navy blue. The solvent was removed by vacuum to leave a blue-purple residue. With use of standard Schlenk techniques, this residue was chromatographed under Ar (alumina III, 20 cm × 2 cm; 90:10 pentane/toluene by volume) at room temperature. The first band was light pink; on evaporation it left a bright red-pink residue of 5 mg (0.009 mmol, 10%) of $[Cp^*RhCO]_2(\mu\text{-}CH_2)$. ^{1}H NMR ($CDCl_3$): found, δ 1.94 (s), 5.95 (s); reported,[22b] δ 1.97 (s), 5.95 (s). IR (C_6H_{12}): found, 1944 cm^{-1}; reported,[22b] 1946 cm^{-1}. Elution with pure toluene gave a blue band which upon evaporation gave 15 mg (0.028 mmol, 30%) of $[Cp^*RhCO]_2$.

$[Cp^*Rh(CO)]_2(CH_2)_3$. All manipulations were performed in the dark. A 100-mL round-bottom flask was charged with 50 mg (0.082 mmol) of $(K^+)_2[Cp^*RhCO]_2{}^{2-}$ and 35 mg (0.091 mmol) of $(TsO)(CH_2)_3(OTs)$ and then connected to a vacuum line. Approximately 5 mL of THF was vacuum distilled onto the solids, and the resulting solution was stirred at room temperature for 0.5 h. The solvent was removed by vacuum to leave a navy blue residue. With use of standard Schlenk techniques, this residue was chromatographed under Ar (alumina III, 20 cm × 2 cm; 90:10 pentane/toluene by volume) at room temperature. The first band was yellow; on evaporation it left an orange residue. Further elution with pure toluene gave a navy blue band which contained $[Cp^*RhCO]_2$. Recrystallization of the orange residue from pentane at −70 °C gave 5 mg (0.009 mmol, 10%) of $[Cp^*RhCO]_2(CH_2)_3$ as a red-orange microcrystalline product. ^{1}H NMR (C_6D_6): δ 1.67 (s, 30 H), 1.33 (t of d, $J_{\text{H-H}} = 6.8$ Hz, $J_{\text{H-Rh}} = 2.3$ Hz, 4 H), 1.10 (quint, $J_{\text{H-H}} = 6.8$ Hz, 2 H). IR (C_6H_{12}): 1782 cm^{-1}. MS: *m/e* = 574 (M^+), 532 ($M^+ - C_3H_6$), 373 ($[Cp^*]_2Rh^+$). Anal. Calcd for $C_{25}H_{36}O_2Rh_2$: C, 52.28; H, 6.32. Found: C, 52.30; H, 6.60.

$[Cp^*Rh(CO)(CH_3)]_2$ from $[Cp^*RhCO]_2{}^{2-}$. All manipulations were performed in the dark. A solution of $(K^+)_2[Cp^*RhCO]_2{}^{2-}$ was generated as described above from 150 mg (0.28 mmol) of $[Cp^*RhCO]_2$. The red solution was filtered; subsequent addition by vacuum transfer of ca. 0.2 mL of CH_3I caused the color to change to navy blue. The solvent was removed under vacuum to leave a navy blue residue. With use of standard Schlenk techniques, this residue was chromatographed under Ar (Alumina III, 25 cm × 2 cm; 90:10 pentane/toluene by volume) at room temperature. A long leading yellow edge came down the column, followed by a compact yellow band. The leading edge and the band were collected separately, and the solutions were evaporated under vacuum. ^{1}H NMR of the leading edge showed the presence of approximately equal amounts of *cis-* and *trans*-$[Cp^*Rh(CO)(CH_3)]_2$. ^{1}H NMR of the band showed the presence of one of the isomers nearly pure; recrystallization of the residue from pentane at −70 °C gave 5 mg (0.008 mmol, 3%) of *cis*-$[Cp^*Rh(CO)(CH_3)]_2$ as an orange microcrystalline product. The product was identified by comparison of its ^{1}H NMR and IR spectra to that of an authentic sample (vide infra).

$[Cp^*{}_2Rh_2(CO)_2(R)]^-$ ($R = CH_3$, C_2H_5, C_6H_5). An H-tube reactor containing a solution of 50 mg (0.094 mmol) of $[Cp^*RhCO]_2$ in approximately 10 mL of THF was stirred at room temperature. This solution was titrated with a 1.6 M solution of CH_3Li in diethyl ether until the color changed from navy blue to dark red (approximately 0.1 mL of the CH_3Li solution was needed). Layering this solution with 5 mL of pentane followed by slow diffusion of the solvent layers led to the isolation of a pink powder. This precipitate decomposed upon redissolution in THF or after exposure to high vacuum for 12 h at room temperature. The above reaction was performed on a small scale to obtain spectral data. ^{1}H NMR (THF-d_8): δ 1.93 (s), 1.74 (s, overlapped with THF-d_8 residual protons), −0.97 ($J_{\text{H-Rh}}$ not observed). In addition a small impurity was observed at δ 1.3 (s). IR (THF): 1755 (m), 1710 (w), 1637 (s, br) cm^{-1}. $[Cp^*{}_2Rh_2(CO)_2(C_2H_5)]^-$ and $[Cp^*{}_2Rh_2(CO)_2(C_6H_5)]^-$ were made analogously. These compounds were generated in situ in subsequent reactions.

***cis*-$[Cp^*Rh(CO)(CH_3)]_2$ from $[Cp^*RhCO]_2$.** A round-bottom flask containing a solution of 200 mg (0.38 mmol) of $[Cp^*RhCO]_2$ in approximately 10 mL of THF was stirred at room temperature. This solution was titrated with a 1.6 M solution of CH_3Li in diethyl ether until the color changed from navy blue to dark red and a pink precipitate formed on the bottom of the flask (approximately 0.4 mL of the CH_3Li solution was needed).

All further manipulations were performed in the dark. The reaction mixture was cooled to −78 °C, 150 μL of CH_3I was added by syringe under Ar, and the resulting solution was stirred for 1 h. The resulting homogeneous orange solution was warmed to 0 °C, and the THF was removed by vacuum to leave an orange residue. The residue was dissolved in toluene at 0 °C; the solution was filtered through a thin (1-cm) pad of alumina III and concentrated to approximately 3 mL. Addition of 3 mL of pentane followed by cooling to −70 °C gave 50 mg of only *cis*-$[Cp^*Rh(CO)(CH_3)]_2$ as determined by ^{1}H NMR. Evaporation of the mother liquor, redissolution of the residue in pentane, concentration of the solution, and cooling to −70 °C gave 75 mg of the same isomer (total yield 125 mg, 0.22 mmol, 59%) as an orange, microcrystalline, spectroscopically pure solid. A small amount of solid was recrystallized again from pentane to obtain a sample that gave satisfactory microanalysis. ^{1}H NMR (toluene-d_8, 0 °C): δ 1.67 (s, 30 H), −0.09 (d, $J_{\text{H-Rh}} = 2.1$ Hz, 6 H). $^{13}C\{^1H\}$ NMR (toluene-d_8, 0 °C): δ 102.1 ($C_5(CH_3)_5$, $J_{\text{C-Rh}}$ not observed), 9.2 (s, $C_5(CH_3)_5$), −6.2 (d, Rh–CH_3, $J_{\text{C-Rh}} = 29$ Hz). IR (C_6H_{12}): 1835 (w), 1793 (s) cm^{-1}. MS: *m/e* 562 (M^+), 532 ($M^+ - C_2H_6$). Anal. Calcd for $C_{24}H_{36}O_2Rh_2$: C, 51.26; H, 6.45. Found: C, 51.53; H, 6.55.

***cis*-$[Cp^*{}_2Rh_2(CO)_2(CH_3)(CD_3)]$.** The procedure was identical with that of the synthesis of $[Cp^*Rh(CO)(CH_3)]_2$ except CD_3I was used in place of CH_3I. Mass spectral data indicated the compound was 90% d_3 and 10% d_0. MS: *m/e* 565 (M^+), 532 ($M^+ - C_2H_3D_3$).

***cis*-$[Cp^*{}_2Rh_2(CO)_2(CH_3)(C_2H_5)]$.** A round-bottom flask containing a solution of 200 mg (0.38 mmol) of $[Cp^*RhCO]_2$ in approximately 10 mL of THF was stirred at room temperature. This solution was titrated with a 1.6 M solution of CH_3Li in diethyl ether until the color changed from navy blue to dark red and a pink precipitate formed on the bottom of the flask (approximately 0.4 mL of the CH_3Li solution was needed).

All further manipulations were performed in the dark. The reaction mixture was cooled to 0 °C, 80 mg (0.40 mmol) of EtOTs was added, and the resulting solution was stirred for 2 h. The THF was removed from the resulting homogeneous orange solution at 0 °C by vacuum to leave an orange-red residue. The residue was chromatographed (alumina III, 20 cm × 2 cm, 90:10 pentane/toluene by volume) at room temperature. An orange band was collected and the solvent removed by vacuum to leave a red-orange residue. Recrystallization from a minimum amount of pentane by slow cooling to −70 °C gave 125 mg (0.22 mmol, 58%) of greater than 85% *cis*-$[Cp^*{}_2Rh_2(CO)_2(CH_3)(C_2H_5)]$ as red-orange needles; the remaining 15% was the trans isomer. A small amount of solid was recrystallized again from pentane to obrain a sample that gave a satisfactory microanalysis. ^{1}H NMR (toluene-d_8, 0 °C): δ 1.69 (s, 15 H), 1.67 (s, 15 H), 1.10 (t, $J_{\text{H-H}} = 7.4$ Hz, 3 H), 0.84 (quart of d, $J_{\text{H-H}} = 7.4$ Hz, $J_{\text{H-Rh}} = 2.4$ Hz, 2 H), −0.09 (d, $J_{\text{H-Rh}} = 2.6$ Hz, 3 H). $^{13}C\{^1H\}$ NMR (toluene-d_8, 0 °C): δ 102.4 ($C_5(CH_3)_5$, $J_{\text{C-Rh}}$ not observed), 102.2 ($C_5(CH_3)_5$, $J_{\text{C-Rh}}$ not observed), 18.7 (s, CH_2CH_3), 9.2 (s, $C_5(CH_3)_5$), 9.0 (s, $C_5(CH_3)_5$), 7.0 (d, CH_2CH_3, $J_{\text{C-Rh}} = 27$ Hz), −6.8 (d, Rh–CH_3, $J_{\text{C-Rh}} = 27$ Hz). IR (C_6H_{12}): 1832 (w), 1788 (s) cm^{-1}. MS: *m/e* 576 (M^+), 546 ($M^+ - C_2H_6$), 532 ($M^+ - C_3H_8$). Anal. Calcd for $C_{25}H_{38}O_2Rh_2$: C, 52.10; H, 6.65. Found: C, 51.98; H, 6.69.

***cis*-$[Cp^*Rh(CO)(C_2H_5)]_2$.** A round-bottom flask containing a solution of 200 mg (0.38 mmol) of $[Cp^*RhCO]_2$ in approximately 10 mL of THF was stirred at room temperature. This solution was titrated with a saturated solution of C_2H_5Li in THF until the color changed from navy blue to dark red.

All further manipulations were performed in the dark. The reaction mixture was cooled to 0 °C, 75 mg (0.37 mmol) of EtOTs was added and the resulting solution was stirred for 2 h. The THF was removed from the resulting red-orange solution at 0 °C by vacuum to leave a red residue. The residue was chromatographed (alumina III, 20 cm × 2 cm, 90:10 pentane/toluene by volume) at room temperature. An orange band was collected and the solvent removed by vacuum to leave a red residue. Recrystallization from a minimum amount of pentane by slow cooling to −70 °C gave 75 mg (0.13 mmol, 34%) of greater than 90% *cis*-$[Cp^*Rh(CO)(CH_2CH_3)]_2$ as red needles; the remaining 10% was the trans isomer. A small amount of solid was recrystallized again from pentane to obtain a satisfactory microanalysis. ^{1}H NMR (toluene-d_8, 0 °C): δ 1.70 (s, 30 H), 1.16 (t, $J_{\text{H-H}} = 7.4$ Hz, 6 H), 0.81 (quart of d, $J_{\text{H-H}} = 7.4$ Hz, $J_{\text{H-Rh}} = 2.3$ Hz, 4 H). $^{13}C\{^1H\}$

NMR (toluene-d_8, 0 °C): δ 102.7 ($C_5(CH_3)_5$, $J_{C\text{-}Rh}$ = 4 Hz), 18.8 (s, CH_2CH_3), 9.2 (s, $C_5(CH_3)_5$), 6.1 (d, CH_2CH_3, $J_{C\text{-}Rh}$ = 27 Hz). IR (C_6H_{12}): 1830 (w), 1797 (s) cm^{-1}. MS: *m/e* 590 (M^+), 560 (M^+ C_2H_6), 532 ($M^+ - C_4H_{10}$). Anal. Calcd for $C_{26}H_{40}O_2Rh_2$: C, 52.89; H, 6.83. Found: C, 53.29; H, 7.14.

***cis*-[Cp*$_2$Rh$_2$(CO)$_2$(C$_6$H$_5$)(CH$_3$)].** A round-bottom flask containing a solution of 200 mg (0.38 mmol) of [Cp*RhCO]$_2$ in approximately 10 mL of THF was stirred at room temperature. This solution was titrated with a saturated solution of C_6H_5Li in THF until the color changed from navy blue to dark red.

All further manipulations were performed in the dark. The reaction mixture was cooled to 0 °C, 80 mg (0.42 mmol) MeOTs was added, and the resulting solution was stirred for 2 h. The THF was removed from the resulting red solution at 0 °C by vacuum to leave a red residue. The residue was dissolved in toluene and quickly filtered through a 1-cm pad of alumina III at room temperature. A red solution was collected and the solvent removed by vacuum to leave a red residue. Recrystallization from a minimum amount of pentane by slow cooling to −70 °C gave 73 mg (0.12 mmol, 31%) of only *cis*-[Cp*$_2$Rh$_2$(CO)$_2$(C$_6$H$_5$)(CH$_3$)] as red needles. A small amount of solid was recrystallized again from pentane to obtain a sample that gave a satisfactory microanalysis. ^{1}H NMR (THF-d_8, 0 °C): δ 7.15 (m, 2 H), 6.7 (two overlapping m, 3 H), 1.79 (s, 15 H), 1.67 (s, 15 H), −1.13 (d, $J_{H\text{-}Rh}$ = 2.5 Hz, 3 H). $^{13}C\{^1H\}$ NMR (THF-d_8, 0 °C): δ 235.6 (t, CO, $J_{C\text{-}Rh}$ = 42 Hz), 148.7 (d, C_6H_5, $J_{C\text{-}Rh}$ = 36 Hz), 138.3 (s, C_6H_5), 127.8 (s, C_6H_5), 123.1 (s, C_6H_5), 103.8 (d, $C_5(CH_3)_5$, $J_{C\text{-}Rh}$ = 5 Hz), 103.3 (d, $C_5(CH_3)_5$, $J_{C\text{-}Rh}$ = 4 Hz), 9.5 (s, $C_5(CH_3)_5$), 9.4 (s, $C_5(CH_3)_5$), −0.3 (d, Rh–CH_3, $J_{C\text{-}Rh}$ = 26 Hz). IR (C_6H_{12}): 1835 (w), 1791 (s) cm^{-1}. MS: *m/e* 624 (M^+), 596 (M^+ − CO), 581 (M^+ − CO − CH_3), 553 (M^+ − 2CO − CH_3), 532 (M^+ − C_6H_5 − CH_3). Anal. Calcd for $C_{29}H_{38}O_2Rh_2$: C, 55.78; H, 6.13. Found: C, 55.87; H, 6.16.

Electrochemical Experiments. All manipulations were performed in the drybox. The experiments were carried out in acetonitrile as solvent and 0.1 M tetrabutylammonium tetrafluoroborate as supporting electrolyte. The solvent was dried over activated 3Å molecular sieves and deoxygenated by several freeze–evacuate–thaw cycles. Cyclic voltammetry of [Cp*RhCO]$_2$ was carried out at a platinum electrode in a solution of CH_3CN and a Ag/0.1 M $AgNO_3$ reference. Under experimental conditions, the reduction potential of ferrocene was −0.055 V relative to the Ag/$AgNO_3$ reference. A one-electron reversible wave (peak to peak separation of 64 mV) was observed at −1.15 V vs. the Ag/$AgNO_3$ reference. In addition, other waves were observed at $E_{1/2}$ = +0.32 and +0.56 V.

Cp*Rh(CO)(CH$_3$)$_2$. A Schlenk flask topped with a rubber septum and equipped with a Teflon covered stir bar was charged with 200 mg (0.32 mmol) of [Cp*RhCl$_2$]$_2$ suspended in ca. 10 mL of toluene. The rubber septum was pierced with a needle connected by a hose to a source of CO. Carbon monoxide was bubbled through the suspension at room temperature for 2 h to afford a red, heterogeneous solution.

This solution was cooled to −78 °C, and 5 mL (10 mmol) of a 2.0 M Me_3Al solution in toluene was added. All the solids were dissolved to give an orange-red solution. Carbon monoxide was bubbled through this solution for another hour at this temperature.

Approximately 2 mL of MeOH was then added to the solution to quench the excess Me_3Al, and the solution was warmed to room temperature. With use of standard Schlenk techniques, the solution was applied to a chromatography column and chromatographed under Ar (Florisil, 20 cm × 2 cm, toluene) at room temperature. An orange-red band was collected, the the solvent was removed under vacuum to leave a red residue. Recrystallization of the residue from pentane at −70 °C left 25 mg (0.084 mmol, 26%) of Cp*Rh(CO)(CH$_3$)$_2$ as a spectroscopically pure red-orange solid. This experiment was not reproducible, and this procedure represents the best yield achieved. ^{1}H NMR (C_6D_6): δ 1.47 (s, 15 H), 0.47 (d, $J_{H\text{-}Rh}$ = 2.3 Hz, 6 H). $^{13}C\{^1H\}$ NMR (C_6D_6): δ 193.5 (d, Rh–CO, $J_{C\text{-}Rh}$ = 78.9 Hz), 100.5 (d, $C_5(CH_3)_5$, $J_{C\text{-}Rh}$ = 2.9 Hz), 8.7 (s, $C_5(CH_3)_5$), −5.0 (d, Rh–CH_3, $J_{C\text{-}Rh}$ = 25.3 Hz). IR (C_6H_{12}): 2000 cm^{-1}.

Reactions of [Cp*Rh(CO)(CH$_3$)]$_2$. All manipulations were performed in the dark. In each reaction an 18 cm long, 5 mm diameter NMR tube fused to a right-angle stopcock with a Teflon valve that could be connected to the vacuum line was charged with 10 mg (0.018 mmol) of [Cp*Rh(CO)(CH$_3$)]$_2$. In the reaction with P(C$_6$H$_5$)$_3$, the tube was also charged with 7 mg (0.027 mmol) of P(C$_6$H$_5$)$_3$. In all cases, the stopcocks were closed and the tubes connected to a vacuum line. NMR solvent (C_6D_6 or toluene-d_8) was vacuum transfered onto the solids so that the solution occupied 5 cm of each NMR tube. In the reactions with gases or volatile liquids, the tubes were pressurized with 300–700 torr of substrate. The tubes were then flame sealed and heated to 46 °C, and the ^{1}H NMR spectra were periodically recorded. In all cases, no intermediates were detected. After time, the tubes were brought into the drybox and opened, the solvent was removed by vacuum, and the residue was dissolved in C_6H_{12} for solution IR analysis. The products were identified by comparison of their IR and/or ^{1}H NMR spectra to those of authentic samples or to literature values.

Kinetics of the Reaction of [Cp*Rh(CO)(CH$_3$)]$_2$ with P(C$_6$H$_5$)$_3$. All manipulations were performed in the dark. In the drybox a standard 0.0445 M solution of [Cp*Rh(CO)(CH$_3$)]$_2$ in toluene-d_8 was prepared by dissolving 25.0 mg (0.0445 mmol) of [Cp*Rh(CO)(CH$_3$)]$_2$ in toluene-d_8, adding a small amount (ca. 10 μL) of hexamethyldisiloxane and bringing the solution volume up to 1.00 mL in a volumetric flask.

Four NMR tubes were fused to an apparatus that had a right angle joint with a Teflon stopcock that could be connected to the vacuum line. The tubes were charged with 12.5 mg (0.0477 mmol), 25.0 mg (0.0953 mmol), 50.0 mg (0.191 mmol), and 125 mg (0.477 mmol) of P(C$_6$H$_5$)$_3$, respectively, and transferred into the drybox. To each of these tubes was added 0.200 mL of the standard solution of [Cp*Rh(CO)(CH$_3$)]$_2$ by volumetric pipet. The phosphine was dissolved at room temperature, the Teflon stopcock was closed, and the apparatus removed from the drybox and connected to the vacuum line. The volume of each solution was brought up to 0.5 mL by vacuum transfer of toluene-d_8. Thus, the solutions were 0.0178 M in [Cp*Rh(CO)(CH$_3$)]$_2$ and 0.0953, 0.191, 0.381, and 0.953 M in P(C$_6$H$_5$)$_3$, respectively. Each solution was frozen, and the tubes were flame sealed under vacuum. ^{1}H NMR spectra of the samples at room temperature showed no detectable reaction of [Cp*Rh(CO)(CH$_3$)]$_2$ with P(C$_6$H$_5$)$_3$ had occurred.

The tubes were placed in a constant temperature (51.0 °C) water bath. After specified times, the tubes were removed from the bath and placed in an ice bath until the ^{1}H NMR spectra could be recorded. Generally, the ^{1}H NMR data were recorded every 120–200 min for the first half of the run and every 400 min for the second half of the run; the spectra were recorded at approximately 20 °C.

One-pulse ^{1}H NMR spectra were recorded; each sample was not pulsed for 3–5 minutes before taking a spectrum to ensure magnetic relaxation. The spectrum of each sample at each time interval was recorded at least twice, and the average value of the integrals was used. The concentration of [Cp*Rh(CO)(CH$_3$)]$_2$ was determined by integrating the metal-bound methyl resonance vs. the hexamethyldisiloxane internal standard.

Plotting the natural logarithm of [Cp*Rh(CO)(CH$_3$)]$_2$ concentration vs. time at the four phosphine concentrations gave straight lines as determined by linear least-squares analysis. For [P(C$_6$H$_5$)$_3$] = 0.0953, 0.191, 0.382, and 0.953 M, the slopes were −6.7 (2) × 10^{-4}, −6.3 (2) × 10^{-4}, −7.3 (2) × 10^{-4}, and −5.2 (2) × 10^{-4}; the correlation coefficients were −0.997, −0.993, −0.989, and −0.982, respectively.

Details of the X-ray Diffraction Study. The structure determination was carried out by Dr. Frederick J. Hollander, staff crystallographer, UC berkeley College of Chemistry X-ray diffraction facility (CHEXRAY).

Small black tabular crystals of $(K^+)_2$[Cp*RhCO]$_2^{2-}$·2THF were obtained by generating a solution of the dianion as described above, layering the solution with pentane, and allowing the solvent layers to slowly diffuse at room temperature. Fragments cleaved from some of these crystals were mounted in capillaries in an inert-atmosphere glovebox, and the capillaries were flame-sealed. Preliminary precession photographs indicated triclinic Laue symmetry and yielded preliminary cell dimensions.

The crystal used for data collection was then transferred to an Enraf-Nonius CAD-4 diffractometer and centered in the beam. Automatic peak search and indexing procedures yielded a triclinic

Table I. Crystal and Data Collection Parameters for $(K^+)_2[Cp^*RhCO]_2^{2-}\cdot 2THF$

(A) Crystal Parameters at 25 °C

a = 12.1653 (13) Å
b = 15.2618 (24) Å
c = 19.2691 (28) Å
α = 84.424 (12)°
β = 87.851 (11)°
γ = 77.837 (11)°
V = 3479.9 (12) Å^3
size of cryst: 0.18 × 0.29 × 0.30 mm
space group: $P\bar{1}$
fw = 754.7 amu
Z = 4
d_{calcd} = 1.44 g cm^{-3}
μ(calcd) = 12.01 cm^{-1}

(B) Data Measurement Parameters[11]

radiation: Mo Kα (λ = 0.71073 Å)
monochromator: highly oriented graphite (2θ = 12.2°)
detector: crystal scintillation counter with PHA
reflctns measd: $+h, \pm k, \pm l$
2θ range: 3→45°
scan type: θ–2θ
scan speed: 0.75→6.7 (θ, deg/min)
scan width: $\Delta\theta = 0.5 + 0.347 \tan\theta$
bkgd: measd over 0.25 ($\Delta\theta$) added to each end of the scan
aperture→crystal: 173 mm
vertical aperture: 3.0 mm
horizontal aperture: 2.0 + 1.0 tan θ mm (variable)
no. of unique reflctns collected: 9065
intensity standards: (840), ($\bar{2}$69), (3, 5, 12); measd every hour of X-ray exposure time; over the data collection period a 22% decrease in intensity was observed
orientatn: three reflections were checked after every 250 measurements; crystal orientatn was redetermined if any of the reflections were offset from their predicted positions by more than 0.1°; reorientatn was necessary three times during data collection

reduced primitive cell. Inspection of the Niggli values revealed no conventional cells of higher symmetry.[31]

The 9065 unique raw intensity data were converted to structure factor amplitudes and their estimated standard deviations by correction for scan speed, background, and Lorentz and polarization effects. Inspection of the intensity standards showed a monotonic isotropic decrease to 0.78 of the original intensity. The data were corrected for this decay. Inspection of the azimuthal scan data showed a variation of I_{min}/I_{max} = 0.88 for the average curve. An empirical correction for absorption, based on the azimuthal scan data, was applied to the intensities.

The structure was solved by Patterson methods and refined via standard least-squares and Fourier techniques. The assumption that the space group was centric was confirmed by the successful solution and refinement of the structure. Due to the large amount of thermal motion in the structure, hydrogen atoms were not located on the final difference Fourier map, and it was not felt that the data justified their inclusion in predicted positions.

The final residuals for 605 variables refined against the 6011 data for which $F^2 > 3\sigma(F)^2$ were R = 4.75%, wR = 7.66%, and GOF = 2.74. The R value for all 9065 data was 9.31%.

The quantity minimized by the least-squares program was $\sum w(|F_o - F_c|)^2$, where w is the weight of a given observation. The p factor, used to reduce the weight of intense reflections, was set to 0.04 in the final cycles of refinement. The analytical forms of the scatterin factor tables for the neutral atoms were used, and all non-hydrogen scattering factors were corrected for both the real and imaginary components of anomalous dispersion.

Inspection of the residuals ordered in ranges of $(\sin\theta)/\lambda$, $|F_o|$, and parity and value of the individual indexes showed no unusual features or trends other than those attributable to the lack of hydrogen atoms in the model. There was no evidence of secondary extinction in the low-angle, high-intensity data. The largest peak in the final difference Fourier map had an electron density of 1.35 e/Å^3 and was located near the inversion center at $^1/_2$, $^1/_2$, 0.

The final cell parameters and specific data collection parameters[32] are given in Table I. Positional parameters are in Table II. Selected interatomic distances are in Table III, and selected interatomic angles are in Table IV. General temperature factor expressions and F_o and F_c were provided as supplementary material to the preliminary communication.[28]

Results and Discussion

Alkali-Metal Reduction of $[Cp^*RhCO]_2$. Reduction of $[Cp^*RhCO]_2$ with Na/Hg or Na/K alloy in tetrahydrofuran at room temperature proceeded with the navy blue solution turning forest green after being stirred for 0.5–1.5 h. After being filtered the solution was layered with pentane; slow diffusion of the pentane layer left $K^+[Cp^*RhCO]_2^-$ as a microcrystalline green-black solid. The potassium ion was also encapsulated with 2,2,2 cryptate to form $[K(crypt)]^+[Cp^*RhCO]_2^-$. The ^1H NMR spectrum of the anion in THF-d_8 showed no resonances attributable to the reduced rhodium species. The IR spectrum of $[K(crypt)]^+[Cp^*RhCO]_2^-$ exhibited a single CO band at 1670 cm^{-1} in THF and a single broad band at 1664 cm^{-1} in the solid state (a band due to some decomposition to $[Cp^*RhCO]_2$ was also observed in both spectra). For comparison, neutral $[Cp^*RhCO]_2$ shows a single CO band at 1736 cm^{-1} in THF; the corresponding cobalt radical anion exhibits a single CO band at 1690 cm^{-1}.

The presence of a single IR band in the anion salt indicated a planar structure in solution for the $Rh_2(CO)_2$ unit similar to that observed for the cobalt system. The IR spectrum of $K^+[Cp^*RhCO]_2^-$ showed two bands at 1631 and 1670 cm^{-1} in THF solution and a single band at 1675 cm^{-1} in the solid state; the extra band was presumably due to contact ion pairing. ESR spectroscopy of the cryptate salt of the radical anion in 2-methyltetrahydrofuran showed a single broad line at room temperature ($\omega_{1/2}$ = 28 G) with g = 2.0704. The lack of observed coupling to the ^{103}Rh (I = $^1/_2$) nuclei was not unusual due to the broadness of the line.[33] Cyclic voltammetric measurements showed the reduction of $[Cp^*RhCO]_2$ to $[Cp^*RhCO]_2^-$ was reversible and occurred at −1.15 V relative to a $Ag/AgNO_3$ couple. The measured magnetic moment of $[K(crypt)]^+[Cp^*RhCO]_2^-$ was 1.83 μ_B which was, within experimental error, the same as the theoretical spin-only value of 1.73 μ_B.

In contrast to the behavior of the analogous cobalt system, reduction of $[Cp^*RhCO]_2$ with Na/K alloy in THF for longer times at room temperature proceeded with the initial navy solution turning forest green and then turning dark red. The solution was filtered and layered with pentane; solvent diffusion led to the isolation of small, black, tabular crystals of the diamagnetic, 34-valence-electron complex $(K^+)_2[Cp^*RhCO]_2^{2-}$ which were dried under high vacuum. The potassium ions of this complex were also encapsulated with 2,2,2 cryptate to form $[K(crypt)^+]_2[Cp^*RhCO]_2^{2-}$. The potassium salt exhibited a single line in its ^1H NMR spectrum at δ 1.920 in THF-d_8; the potassium–cryptate salt exhibited this line plus other resonances due to the cryptate. The IR spectrum of $(K^+)_2[Cp^*RhCO]_2^{2-}$ in THF solution in the CO region consisted of five moderately broad bands at 1747, 1690, 1669, 1635, and 1588 cm^{-1}. The IR spectrum in THF solution of $[K(crypt)^+]_2[Cp^*RhCO]_2^{2-}$ showed bands at 1694 and 1669 cm^{-1} and a weak band at 1743 cm^{-1}. The

---

(31) Details of the diffraction equipment and data reduction formulae used are given in ref 8h.

(32) (a) Unit cell parameters and their esds were derived by a least-squares fit to the setting angles of the unresolved Mo Kα components of 24 reflections with 2θ near 28°. (b) In the X-ray data tables the esds of all parameters are given in parentheses, right justified to the least significant digit(s) given.

(33) (a) Wayland, B. B.; Newman, A. R. *Inorg. Chem.* **1981**, *20*, 3093. (b) Van Gaal, H. L. M.; Verlaak, J. M. J.; Posno, T. *Inorg. Chim. Acta* **1977**, *23*, 43.

Table II. Positional Parameters and Their Estimated Standard Deviations[c]

atom	*x*	*y*	*z*	*B*, Å^2	atom	*x*	*y*	*z*	*B*, Å^2
Rh1	0.19841 (8)	0.03335 (6)	0.31740 (4)	4.06 (2)	C31	0.488 (1)	0.4531 (8)	0.3513 (6)	5.4 (3)
Rh2	0.29995 (8)	0.02947 (5)	0.19556 (4)	3.62 (2)	C32	0.501 (1)	0.3669 (9)	0.3839 (6)	5.7 (3)
Rh3	0.39944 (8)	0.36266 (6)	0.28649 (4)	3.59 (2)	C33	0.568 (1)	0.3059 (8)	0.3350 (7)	6.6 (3)
Rh4	0.20270 (8)	0.41672 (5)	0.22956 (4)	3.47 (2)	C34	0.592 (1)	0.3588 (9)	0.2733 (7)	5.7 (3)
K1	0.0512 (2)	0.2603 (2)	0.3139 (1)	5.19 (7)	C35	0.542 (1)	0.4496 (8)	0.2858 (7)	5.5 (3)
K2	0.2019 (2)	0.2497 (2)	0.1136 (1)	4.79 (6)	C36	0.425 (2)	0.538 (1)	0.3816 (9)	11.9 (5)
K3	0.4993 (2)	0.1592 (2)	0.2088 (1)	4.74 (6)	C37	0.464 (2)	0.341 (1)	0.4583 (7)	12.7 (6)
K4	0.3397 (3)	0.1698 (2)	0.4040 (1)	5.85 (8)	C38	0.625 (1)	0.205 (1)	0.354 (1)	11.1 (5)
O1	0.4362 (7)	0.0521 (5)	0.3135 (4)	4.9 (2)	C39	0.668 (1)	0.326 (1)	0.2112 (8)	8.6 (5)
O2	0.0847 (7)	0.1628 (5)	0.2041 (4)	4.8 (2)	C40	0.553 (1)	0.533 (1)	0.2341 (9)	9.7 (5)
O3	0.3810 (6)	0.3090 (5)	0.1463 (4)	4.5 (2)	C41	0.083 (1)	0.5534 (8)	0.2409 (7)	7.6 (4)
O4	0.2042 (7)	0.3279 (5)	0.3724 (4)	5.2 (2)	C42	0.019 (1)	0.4907 (9)	0.2302 (7)	6.2 (3)
O5	−0.0911 (8)	0.3270 (6)	0.4192 (5)	7.4 (3)	C43	0.042 (1)	0.4617 (8)	0.1666 (7)	5.4 (3)
O6	0.160 (1)	0.2902 (7)	−0.0310 (5)	8.7 (3)	C44	0.120 (1)	0.5028 (8)	0.1334 (6)	5.3 (3)
O7	0.7030 (9)	0.1275 (7)	0.1378 (6)	9.8 (3)	C45	0.150 (1)	0.5639 (7)	0.1774 (8)	6.6 (4)
O8	0.325 (1)	0.1825 (8)	0.5463 (5)	9.0 (3)	C46	0.084 (2)	0.611 (1)	0.3034 (9)	17.1 (7)
C1	0.3486 (9)	0.0469 (7)	0.2868 (5)	3.9 (3)	C47	−0.079 (1)	0.468 (1)	0.280 (1)	12.5 (6)
C2	0.163 (1)	0.1050 (6)	0.2283 (5)	4.0 (3)	C48	−0.027 (1)	0.407 (1)	0.129 (1)	10.1 (5)
C3	0.3432 (9)	0.3421 (6)	0.1984 (5)	3.4 (2)	C49	0.167 (2)	0.493 (1)	0.0587 (8)	11.3 (6)
C4	0.2489 (9)	0.3537 (7)	0.3166 (5)	3.7 (2)	C50	0.231 (2)	0.627 (1)	0.163 (1)	15.6 (8)
C11	0.184 (1)	−0.1005 (8)	0.3872 (7)	6.8 (4)	C51	−0.213 (2)	0.351 (1)	0.4193 (9)	9.6 (5)[a]
C12	0.081 (1)	−0.0685 (8)	0.3560 (7)	6.8 (4)	C52	−0.247 (2)	0.443 (1)	0.444 (1)	12.3 (6)[a]
C13	0.037 (1)	0.0180 (9)	0.3791 (7)	6.5 (3)	C53	−0.150 (2)	0.448 (1)	0.491 (1)	11.5 (6)[a]
C14	0.114 (1)	0.0391 (8)	0.4271 (6)	6.1 (3)	C54	−0.055 (1)	0.364 (1)	0.4775 (9)	8.9 (4)[a]
C15	0.212 (1)	−0.0361 (8)	0.4312 (6)	7.0 (4)	C61	0.241 (2)	0.321 (1)	−0.083 (1)	11.7 (6)[a]
C16	0.263 (2)	−0.191 (1)	0.379 (1)	10.8 (6)	C62	0.201 (2)	0.310 (1)	−0.151 (1)	10.9 (5)[a]
C17	0.019 (2)	−0.117 (1)	0.3098 (9)	10.3 (5)	C63	0.131 (2)	0.257 (1)	−0.146 (1)	12.6 (7)[a]
C18	−0.082 (1)	0.077 (1)	0.3679 (9)	8.8 (5)	C64	0.067 (2)	0.274 (1)	−0.069 (1)	10.7 (5)[a]
C19	0.088 (1)	0.1126 (9)	0.4770 (6)	6.9 (4)	C71	0.725 (2)	0.176 (2)	0.077 (1)	14.2 (8)[a]
C20	0.314 (2)	−0.048 (1)	0.4770 (7)	9.6 (5)	C72	0.867 (2)	0.153 (1)	0.089 (1)	11.9 (6)[a]
C21	0.381 (1)	−0.1074 (7)	0.1488 (6)	5.3 (3)	C73	0.907 (2)	0.069 (2)	0.125 (1)	16.6 (9)[a]
C22	0.453 (1)	−0.0421 (7)	0.1315 (6)	4.7 (3)	C74	0.805 (3)	0.072 (2)	0.168 (2)	18 (1)
C23	0.390 (1)	0.0326 (7)	0.0870 (5)	4.4 (3)	C81	0.249 (2)	0.259 (1)	0.575 (1)	11.9 (6)[a]
C24	0.281 (1)	0.0127 (7)	0.0777 (5)	4.6 (3)	C82	0.286 (2)	0.273 (2)	0.641 (1)	17.1 (9)[a]
C25	0.278 (1)	−0.0739 (7)	0.1152 (6)	5.0 (3)	C83	0.323 (3)	0.190 (2)	0.667 (2)	18 (1)
C26	0.418 (1)	−0.1994 (8)	0.1906 (7)	7.8 (4)	C84	0.374 (2)	0.130 (2)	0.613 (1)	13.8 (7)[a]
C27	0.574 (1)	−0.055 (1)	0.1514 (8)	6.7 (4)	Cp1	0.1257	−0.0296	0.3962	*b*
C28	0.439 (1)	0.1040 (7)	0.0453 (6)	5.5 (3)	Cp2	0.3563	−0.0355	0.1120	*b*
C29	0.194 (1)	0.0654 (9)	0.0323 (6)	6.0 (3)	Cp3	0.5382	0.3869	0.3260	*b*
C30	0.178 (1)	−0.1192 (8)	0.1168 (7)	7.2 (4)	Cp4	0.0900	0.5145	0.1898	*b*

[a] Atoms refined with isotropic thermal parameters. [b] Cp1 etc. are the centroids of the cyclopentadiene rings. [c] Anisotropically refined atoms are given in the form of the isotropic equivalent thermal parameter defined as $(^4/_3)$ $[a^2\beta(1.1) + b^2\beta(2.2) + c^2\beta(3.3) + ab(\cos\gamma)\beta(1.2) + ac(\cos\beta)\beta(1.3) + bc(\cos\alpha)\beta(2.3)]$.

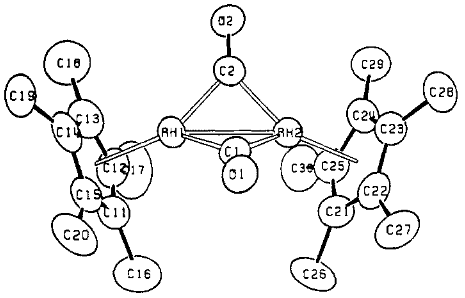

Figure 1. ORTEP diagram of one of the dirhodium units in $(K^+)_2[Cp^*RhCO]_2^{2-}\cdot 2THF$ showing orientation of the carbonyl and pentamethylcyclopentadienyl units.

solid-state IR spectra of these dianions were extremely broad and featureless.

Determination of the Structure of $(K^+)_2[Cp^*RhCO]_2^{2-}\cdot 2THF$ by X-ray Diffraction. A crystal of the potassium salt of the dianion was isolated as described above but not dried under vacuum. An X-ray crystallographic analysis carried out at room temperature determined both the solid-state structure of the molecule and its stoichiometry as $(K^+)_2[Cp^*RhCO]_2^{2-}\cdot 2THF$. Solution of the structure revealed that the crystal contains dianion molecules associated in pairs, joined by aggregates of four potassium atoms. The overall complex adopted idealized D_{2d} symmetry. Figure 1 shows an ORTEP diagram of one of the dirhodium units, with its carbonyl and pentamethylcyclopentadienyl ligands. Figures 2 and 3 show two views of the dimeric complex. These latter figures show how two dirhodium species are linked through their carbonyl oxygen atoms to an idealized square of potassium

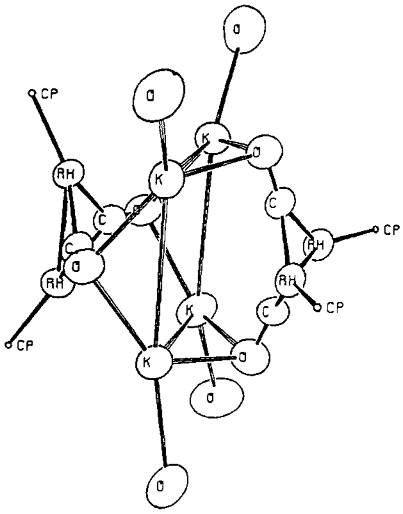

Figure 2. ORTEP diagram of $(K^+)_2[Cp^*RhCO]_2^{2-}\cdot 2THF$ showing how the two dirhodium units in the asymmetric unit are linked together through a square array of potassium ions (carbon atoms of the THF groups and Cp* rings removed for clarity).

Table III. Selected Interatomic Distances[a]

atom 1	atom 2	distance
Rh1	Rh2	2.606 (1)
C1	Rh1	1.942 (8)
C1	Rh2	1.939 (8)
C1	O1	1.224 (8)
C2	Rh1	1.955 (7)
C2	Rh2	1.932 (7)
C2	O2	1.231 (8)
Rh1	C11	2.368 (7)
Rh1	C12	2.370 (8)
Rh1	C13	2.290 (8)
Rh1	C14	2.311 (8)
Rh1	C15	2.337 (8)
Rh1	Cp1	1.993
Rh2	C21	2.360 (7)
Rh2	C22	2.322 (7)
Rh2	C23	2.321 (7)
Rh2	C24	2.336 (6)
Rh2	C25	2.378 (7)
Rh2	Cp2	1.994
Rh3	Rh4	2.613 (1)
C3	Rh3	1.934 (6)
C3	Rh4	1.951 (7)
C3	O3	1.199 (7)
C4	Rh3	1.926 (7)
C4	Rh4	1.896 (7)
C4	O4	1.251 (7)
Rh3	C31	2.387 (8)
Rh3	C32	2.305 (7)
Rh3	C33	2.252 (8)
Rh3	C34	2.339 (8)
Rh3	C35	2.390 (8)
Rh3	Cp3	1.998
Rh4	C41	2.302 (8)
Rh4	C42	2.287 (8)
Rh4	C43	2.289 (8)
Rh4	C44	2.300 (7)
Rh4	C45	2.340 (7)
Rh4	Cp4	1.923
K1	O2	2.673 (5)
K1	O4	2.648 (5)
K1	O5	2.740 (6)
K2	O2	2.640 (5)
K2	O3	2.650 (5)
K2	O6	2.840 (7)
K3	O1	2.662 (5)
K3	O3	2.641 (5)
K3	O7	2.754 (8)
K4	O1	2.682 (5)
K4	O4	2.652 (5)
K4	O8	2.763 (6)
K1	K2	4.205 (2)
K2	K3	4.040 (2)
K3	K4	4.162 (2)
K4	K1	3.905 (3)
K1	Rh1	3.544 (2)
K1	Rh4	3.548 (2)
K2	Rh2	3.556 (2)
K2	Rh4	3.551 (2)
K3	Rh2	3.469 (2)
K3	Rh3	3.539 (2)
K4	Rh1	3.535 (2)
K4	Rh3	3.714 (2)

[a] Cp1–Cp4 are the centroids of the cyclopentadiene rings.

atoms (nonbonding K–K distances of 4.205 (2), 4.040 (2), 4.162 (2), and 3.905 (3) Å). The dianions are rotated by 90° relative to each other so that all four edges of the K_4 unit are identically bridged by carbonyl oxygen atoms. The coordination sphere of each potassium atom is completed by the oxygen of a THF molecule of solvation. The

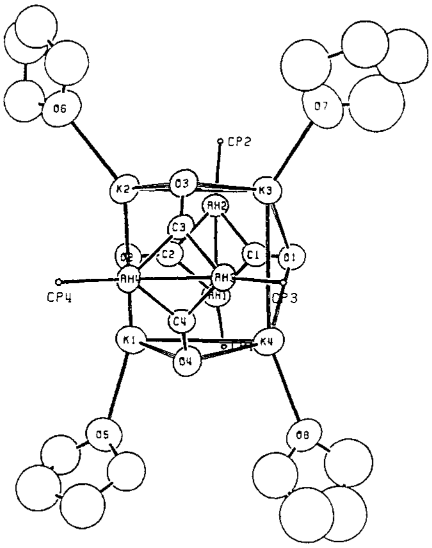

Figure 3. Alternative view of $(K^+)_2[Cp^*RhCO]_2^{2-}\cdot 2THF$ down the pseudo-S_4 axis, illustrating the relationship of the tetrarhodium/dipotassium unit to the four THF molecules of solvation.

Rh–Rh distances are 2.606 (1) and 2.613 (1) Å; the lower formal metal–metal bond order is reflected by an increase of the metal–metal bond length compared to the metal–metal bond distance of 2.564 Å in neutral $[Cp^*RhCO]_2$.[14] The average Rh–Rh–CO dihedral angle was 124° and the centroids of the Cp* ligands were skewed from the Rh–Rh vector by an average of 30°.

Although there are steric constraints enforced by this potassium coordination that might require the observed bending, the dianion may still be bent in the absence of coordinating cations. In fact, the nonbonding nature of the potassium–potassium distances and the unusual three-coordinate geometry of the potassium atoms indicated that the potassium coordination was dictated by dianion geometry, rather than the reverse. In addition, more than one IR band in solution was observed for the CO ligands of the noncoordinating cation salt $[K(crypt)]_2^+[Cp^*RhCO]_2^{2-}$, and the isoelectronic $[CpNiCO]_2$ has a nonplanar $Ni_2(CO)_2$ framework.[34] These data suggest that the free dianion is bent.[35]

Extended Hückel calculations that predict this bending have been performed. The results for $[CpCoCO]_2$[36] and $[CpRhCO]_2$[37] are qualitatively similar, and the orbital ordering and energies are confirmed by photoelectron spectroscopy.[38] The calculations indicate the two highest occupied orbitals of $[CpMCO]_2$, orbitals of a_1 and a_2 symmetry, are destabilized when the CO ligands are bent out of a coplanar arrangement with the M atoms. Thus, $[CpMCO]_2$ is predicted to be flat, which is consistent with the experimental observations.

Conversely, the calculations show that upon reduction of $[CpMCO]_2$ a bent configuration becomes favored. The additional electrons are placed in an orbital of b_2 symmetry. This orbital is stabilized through an interaction

---

(34) Madach, T.; Fischer, K.; Vahrenkamp, H. *Chem. Ber.* **1980**, *113*, 3235.

(35) We had hoped to test this conclusion by obtaining an X-ray crystallographic analysis of a noncoordinating cation salt of $[Cp^*RhCO]_2^{2-}$. Unfortunately, suitable crystals of either the bis-PPN$^+$ salt or the bis-$[K(crypt)]^+$ salt could not be obtained.

(36) (a) Pinhas, A. R.; Hoffmann, R. *Inorg. Chem.* **1979**, *18*, 654. (b) Bellagamba, V.; Gamba, A. *J. Organomet. Chem.* **1981**, *212*, 125.

(37) Pinhas, A. R.; Albright, T. A.; Hofmann, P.; Hoffmann, R. *Helv. Chim. Acta* **1980**, *63*, 29.

(38) Dudeney, N.; Green, J. C.; Kirchener, O. N.; Smallwood, F. S. *J. Chem. Soc., Dalton Trans.* **1984**, 1883.

Table IV. Selected Interatomic Angles (deg)

atom 1	atom 2	atom 3	angle	atom 1	atom 2	atom 3	angle
Cp1	Rh1	Rh2	149.21	O2	K1	O4	126.20 (17)
Cp1	Rh1	C1	138.36	O2	K1	O5	147.80 (18)
Cp1	Rh1	C2	141.23	O4	K1	O5	85.78 (18)
C1	Rh1	C2	80.3 (3)	O2	K2	O3	123.87 (16)
Cp2	Rh2	Rh1	150.04	O2	K2	O6	125.94 (21)
Cp2	Rh2	C1	140.32	O3	K2	O6	110.18 (20)
Cp2	Rh2	C2	138.71	O1	K3	O3	128.55 (16)
C1	Rh2	C2	80.9 (3)	O1	K3	O7	125.61 (23)
Rh1	C1	Rh2	84.4 (3)	O3	K3	O7	105.75 (23)
Rh1	C1	O1	137.7 (5)	O1	K4	O4	126.19 (16)
Rh2	C1	O1	137.3 (5)	O1	K4	O8	138.98 (19)
Rh1	C2	Rh2	84.2 (3)	O4	K4	O8	94.79 (19)
Rh1	C2	O2	136.8 (6)	O5	K1	K2	158.09 (15)
Rh2	C2	O2	138.4 (5)	O5	K1	K4	104.21 (14)
Cp3	Rh3	Rh4	151.71	K2	K1	K4	92.23 (5)
Cp3	Rh3	C3	139.88	O6	K2	K1	143.95 (17)
Cp3	Rh3	C4	138.84	O6	K2	K3	128.70 (17)
C3	Rh3	C4	81.2 (3)	K1	K2	K3	87.19 (5)
Cp4	Rh4	Rh3	148.47	O7	K3	K2	123.36 (20)
Cp4	Rh4	C3	136.89	O7	K3	K4	145.52 (20)
Cp4	Rh4	C4	141.11	K2	K3	K4	90.96 (5)
C3	Rh4	C4	81.5 (3)	O8	K4	K1	112.35 (16)
Rh3	C3	Rh4	84.5 (3)	O8	K4	K3	155.65 (18)
Rh3	C3	O3	137.2 (6)	K3	K4	K1	89.60 (5)
Rh4	C3	O3	137.7 (5)				
Rh3	C4	Rh4	86.2 (3)				
Rh3	C4	O4	135.2 (5)				
Rh4	C4	O4	138.0 (6)				

with the π^* orbitals on the CO ligands that occurs upon bending. Furthermore, if the Cp ligands are canted so that their centroids are no longer linear with the M–M bond vector, a bent $M_2(CO)_2$ framework becomes much more favored. In particular, the theoretical studies[37] predict that for a Cp–M–M–Cp configuration skewed by 28°, the $M_2(CO)_2$ dihedral angle should be approximately 130°. These predictions are quite similar to the experimentally observed geometry.

Alkylation Reactions of $[Cp^*RhCO]_2^-$ and $[Cp^*RhCO]_2^{2-}$. These reduced species underwent alkylation reactions analogous to those observed in the cobalt system, although yields in the rhodium case were poor. Both $[Cp^*RhCO]_2^-$ and $[Cp^*RhCO]_2^{2-}$ were treated with a variety of α,ω-diiodides or dioxytosylates to give metallacycles as shown in eq 1.

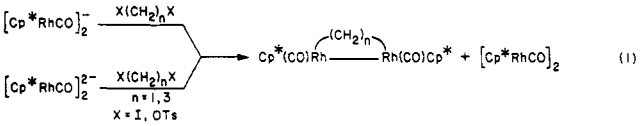

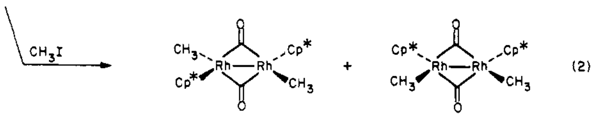

Reaction of either the radical anion or the dianion with CH_2Cl_2 gave the known $[Cp^*_2Rh_2(CO)_2](\mu\text{-}CH_2)$[22] in 10% yield. Reaction of either the radical anion or the dianion with $TsO(CH_2)_3OTs$ gave the new dimetallacyclopentane $[Cp^*_2Rh_2(CO)_2](CH_2)_3$ in 10% yield. Finally, reaction of $[Cp^*RhCO]_2^-$ with $TsO(C_2H_4)OTs$ cleanly gave $[Cp^*RhCO]_2$ and ethylene as the only observable products in the ^1H NMR. In all these alkylations, $[Cp^*RhCO]_2$ was formed as a side product. The compounds were isolated and purified by chromatography on alumina III under air-free conditions.

$[Cp^*RhCO]_2^-$ and $[Cp^*RhCO]_2^{2-}$ were also alkylated with CH_3I to give the cis and trans isomers of $[Cp^*Rh(CO)(CH_3)]_2$ as shown in eq 2. This reaction occurred in only 3% overall yield; $[Cp^*RhCO]_2$ was again produced as a side product.

Due to the poor yields of these alkylation reactions, a different method for preparing the dialkyl complexes was sought. It has been shown that phosphine ligands add unsymmetrically across the double bond of $[CpMCO]_2$ (M = Co[9d,h] or Rh[25]); eq 3 shows the rhodium case. We decided to attempt the analogous metal–carbon bond-forming reaction by treating $[Cp^*RhCO]_2$ with alkyllithium reagents. The reaction shown in eq 4 proceeded immediately at room temperature. With CH_3Li, the navy blue solution turned dark red. The monoalkylated monoanion $[Cp^*_2Rh_2(CO)_2(CH_3)]^-$ was extremely air- and moisture-sensitive, and neither its lithium salt nor its [Li(12-crown-4)]$^+$ salt gave satisfactory microanalysis. Spectral data in THF for the Li^+ salt (^1H NMR δ 1.93 (s), 1.74 (s), −0.97 (J_{H-Rh} not observed); IR 1755 (m), 1710 (w), 1637 (s, br) cm^{-1}) were consistent with the formulation as the unsymmetrical monoadduct. Overall, this unique[39] reaction

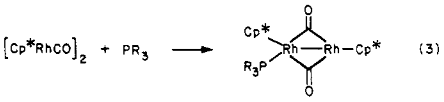

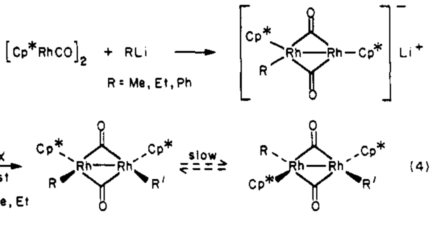

---

[39] Alkyllithium reagents have been added across a metal–metal single bond; the dinuclear complex was held together by a bridging phosphide ligand. (a) Mercer, W. C.; Whittle, R. R.; Burkhardt, E. W.; Geoffroy, G. L. *Organometallics* **1985**, *4*, 68. **Note added in proof**: after submission of this manuscript, analogous reactions in the dimolybdenum system were reported: (b) Mercer, R. J.; Green, M.; Orpen, A. G. *J. Chem. Soc., Chem. Commun.* **1986**, 567.

afforded formal oxidation of one metal center and concomitant reduction of the other metal center.

The chemistry of $[Cp^*{}_2Rh_2(CO)_2(CH_3)]^-$ further supported the proposed structure. Reaction of $[Cp^*{}_2Rh_2(CO)_2(CH_3)]^-$ with CH_3I gave only one isomer of $[Cp^*Rh(CO)(CH_3)]_2$ in 58% isolated yield, as is also shown in eq 4. Unlike the alkylations of $[Cp^*RhCO]_2^-$ or $[Cp^*RhCO]_2^{2-}$, this reaction proceeded with high stereoselectivity in good yield.

Following a similar route, reaction of $[Cp^*RhCO]_2$ with CH_3Li followed by CH_3CH_2OTs gave only one isomer of the unsymmetrical dialkyl complex $[Cp^*{}_2Rh_2(CO)_2(CH_3)(CH_2CH_3)]$, a material which could not be obtained by simple alkylation of $[Cp^*RhCO]_2^-$ or $[Cp^*RhCO]_2^{2-}$. Reaction of $[Cp^*RhCO]_2$ with CH_3CH_2Li followed by treatment of the resulting anion with CH_3CH_2OTs or reaction with C_6H_5Li followed by CH_3OTs gave $[Cp^*Rh(CO)(CH_2CH_3)]_2$ and $[Cp^*{}_2Rh_2(CO)_2(C_6H_5)(CH_3)]$, respectively. All these dialkyl complexes were fully characterized by ^1H and ^{13}C NMR, solution IR, and mass spectroscopy, as well as microanalysis; details are given in the Experimental Section.

In addition to affording improved yields and mixed alkyl complexes, this reaction sequence accomplished control of product stereochemistry as shown in eq 4. Initial alkylation of $[Cp^*{}_2Rh_2(CO)_2R]^-$ at 0 °C in all cases gave predominantly one isomer of $[Cp^*{}_2Rh_2(CO)_2RR']$. Allowing toluene or benzene solutions of these complexes to stand at room temperature slowly gave equilibrium mixtures of both the cis and trans isomers; the newly formed isomer predominated at equilibrium. The mechanism of this interconversion must not involve fragmentation of the dimer into two 17-electron $[Cp^*Rh(CO)R]\cdot$ moieties: isomerization of $[Cp^*{}_2Rh_2(CO)_2(CH_3)(CH_2CH_3)]$ occurs without formation of either $[Cp^*Rh(CO)(CH_3)]_2$ or $[Cp^*Rh(CO)(CH_2CH_3)]_2$.

In these reactions, the first formed dialkyl compound is probably the cis isomer. In all cases, this isomer shows two IR bands for the CO ligands. Conversely, the subsequently formed isomer of $[Cp^*Rh(CO)(CH_3)]_2$ and $[Cp^*{}_2Rh_2(CO)_2(CH_3)(CH_2CH_3)]$ showed only one CO band in the IR spectrum; the thermodynamic isomers of $[Cp^*Rh(CO)(CH_2CH_3)]_2$ and $[Cp^*{}_2Rh_2(CO)_2(C_6H_5)(CH_3)]$ have not yet been isolated. Group theory predicts that *cis*-$[Cp^*Rh(CO)(CH_3)]_2$ (C_{2v} symmetry) would have two CO stretching absorptions in the IR while *trans*-$[Cp^*Rh(CO)(CH_3)]_2$ (C_{2h} symmetry) would have only one.

The thermodynamic isomers of $[Cp^*Rh(CO)(CH_3)]_2$. $[Cp^*{}_2Rh_2(CO)_2(CH_3)(CH_2CH_3)]$, and $[Cp^*{}_2Rh_2(CO)_2(CH_3)(C_6H_5)]$ all showed essentially identical chemical shifts in the ^1H NMR (C_6D_6 solvent) for the protons in the rhodium-bound methyl group: δ −0.42, −0.43, and −0.42, respectively. We assign the trans stereochemistry to these complexes, because the methyl groups are located in each case next to a Cp* ring, and thus their environments are very similar. In contrast, the kinetic isomers exhibit a larger spread in these shifts (δ 0.00, −0.01, and −0.59, respectively). We tentatively assign the opposite (cis) stereochemistry to these species, since here the methyl group is located proximate to a methyl, ethyl, and phenyl group in the three cis compounds.

We believe steric effects play a major role in determining the stereochemistry of both the kinetic and thermodynamic products of this reaction. To account for the predominant formation of the cis complex as the initial (kinetic) product, we assume the alkylation reaction is quite exothermic and is thus characterized by an "early" or reactant-like transition state. Proposed early transition states (i.e., little Rh···R bonding and R···OTs bond cleavage) for formation of cis and trans product are shown as A and B at the top of Scheme III. Because little movement of the Cp* group at the reacting metal center has occurred as yet, most of the steric repulsion occurs between the incoming ROTs molecule and the group located syn to it attached the other metal atom. The CH_3 group is smaller than Cp*, and A is favored, leading to the cis compound. In a "late", or product-like, transition state (C and D), and even more strongly in the final products themselves, the Rh–Rh–Cp* angle has decreased substantially, increasing the steric repulsion between the Cp* group at the reacting rhodium atom and the group attached to the other metal center. In this case the Cp*···Cp* interaction produces a greater repulsion than the Cp*···CH_3 interaction, and the trans complex (which keeps the largest groups farthest apart) is energetically favored.

Scheme III

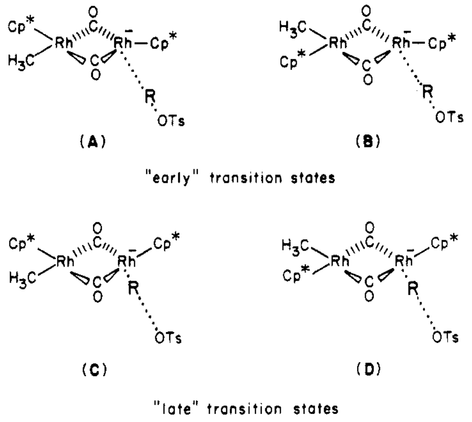

Attempts to extend this chemistry to the preparation of hydrides and secondary alkyl complexes have been unsucessful. Reaction of $[Cp^*RhCO]_2$ with $K[B(O\text{-}i\text{-}Pr)]H$ gave a red solution, but addition of either CH_3OTs or H^+ (as H_2O or CH_3OH) led only to the isolation of $[Cp^*RhCO]_2$, even when the reaction was carried out at −78 °C. Reaction of $[Cp^*RhCO]_2$ with CH_3Li followed by either H_2O or CH_3OH at −78 °C also led only to the isolation of $[Cp^*RhCO]_2$. Likewise, the reaction of $[Cp^*RhCO]_2$ with CH_3Li followed by *i*-PrOTs gave only $[Cp^*RhCO]_2$; surprisingly, *i*-PrLi did not react with $[Cp^*RhCO]_2$ at room temperature. Reaction of $[Cp^*RhCO]_2$ with *i*-PrMgBr followed by CH_3OTs at 0 °C gave a complex mixture of products. Treatment of $[Cp^*RhCO]_2$ with C_6H_5Li followed by C_6H_5I gave a small amount (approximately 10–20%) of an inseparable mixture of $[Cp^*RhCO]_2$ and a complex whose ^1H NMR and IR spectral data were consistent with its formulation as $[Cp^*Rh(CO)(C_6H_5)]_2$. Reaction of $[Cp^*RhCO]_2$ with C_6H_5Li followed by $C_6H_5N_2{}^+PF_6$ gave $[Cp^*RhCO]_2$ as the only tractable product.

Attempts to extend this chemistry to include complexes with metal–nitrogen or metal–oxygen bonds were also unsucessful. Reaction of $[Cp^*RhCO]_2$ with $LiN(C_2H_5)_2$ gave a red solution, but further reaction with CH_3OTs left only $[Cp^*RhCO]_2$. No reaction of $[Cp^*RhCO]_2$ with $LiOCH_3$ was observed even after 1 week at room temperature in THF; the reaction mixture did not change after the addition of 12-crown-4. No reaction of $[Cp^*RhCO]_2$ with KO-*t*-Bu in THF was observed at room temperature. Addition of 2,2,2-cryptate to this mixture gave a green solution. From this solution, dark green crystals were isolated whose IR spectrum and (lack of a) ^1H NMR spectrum were consistent with formulation as $[K(crypt)]^+[Cp^*RhCO]_2^-$.

Chemistry of $[Cp^*Rh(CO)(CH_3)]_2$. In contrast to the dinuclear dialkyl complexes of cobalt which thermally decompose at room temperature,[8] the dinuclear dialkyl complexes of rhodium are thermally quite stable and decompose only slowly at temperatures above 50 °C. In order to determine the chemistry of these rhodium complexes, we chose initially to study the reactivity of $[Cp^*Rh(CO)(CH_3)]_2$.

A number of exploratory reactions of $[Cp^*Rh(CO)(CH_3)]_2$ were performed by monitoring the reaction by ^1H NMR in a sealed tube. Although most of these reactions were quite complicated, some of the products that have been prepared previously were identified by comparison of their ^1H NMR and IR spectral data to those of authentic samples or to literature values. We also attempted to independently synthesize the previously unknown $Cp^*Rh(CO)(CH_3)_2$.[40]

Photolysis of $[Cp^*Rh(CO)(CH_3)]_2$ gave a 1:1 mixture of $[Cp^*RhCO]_2$ and $Cp^*Rh(CO)(CH_3)_2$ and a significant decomposition peak at δ 1.40. Reaction of $[Cp^*Rh(CO)(CH_3)]_2$ with H_2 gave CH_4, approximately equal amounts of $Cp^*Rh(CO)_2$[42] and $[Cp^*RhCO]_2$, and a large amount (50% by integration of the ^1H NMR spectrum) of decomposition. Reaction of $[Cp^*Rh(CO)(CH_3)]_2$ with acetylene deposited large amounts of polymeric material. The reactions of $[Cp^*Rh(CO)(CH_3)]_2$ with dative ligands, however, were more straightforward. The general scheme for this reaction is shown in eq 5. Reaction of $[Cp^*Rh(CO)(CH_3)]_2$ with CO initially gave a 1:1 mixture of $Cp^*Rh(CO)_2$ and $Cp^*Rh(CO)(CH_3)_2$. At longer reaction times, however, a 2:1 mixture of $Cp^*Rh(CO)_2$ and $Cp^*Rh(CO)(CH_3)_2$ was obtained. Presumably, the relative amounts changed due to further reaction of $Cp^*Rh(CO)(CH_3)_2$ with CO.

$$[Cp^*Rh(CO)(CH_3)]_2 + L \longrightarrow Cp^*Rh(L)(CH_3)_2 + Cp^*Rh(CO)_2 \qquad (5)$$

Reaction of $[Cp^*Rh(CO)(CH_3)]_2$ with C_2H_4 gave $Cp^*Rh(CO)_2$, $Cp^*Rh(C_2H_4)_2$,[43] a compound whose ^1H NMR spectral data at 20 °C (δ 1.36 (s), 0.19 (d, J_{H-Rh} = 2.2Hz)) were consistent with formulation as $Cp^*Rh(C_2H_4)(CH_3)_2$,[41a,b] and another large peak at δ 1.71. Reaction with excess $P(CH_3)_3$ gave compounds whose ^1H NMR and IR spectral data were consistent with formulation as $Cp^*Rh(CO)[P(CH_3)_3]$[44] and $Cp^*Rh[P(CH_3)_3](CH_3)_2$ and other unidentified products. The presence of $Cp^*Rh(C_2H_4)_2$ in the former reaction was probably due to further reaction of $Cp^*Rh(C_2H_4)(CH_3)_2$ with C_2H_4. The $Cp^*Rh(CO)[P(CH_3)_3]$ produced in the latter reaction was probably formed by substitution of one of the CO ligands on $Cp^*Rh(CO)_2$ with $P(CH_3)_3$.

It was mentioned in the Introduction that treatment of $[Cp^*Co(CO)(CH_3)]_2$ with PPh_3 led to a complex mixture of products but that the corresponding reaction of its CH_2-linked-ring relative $[C_5H_4)CH_2(C_5H_4)][Co(CO)(CH_3)]_2$ gave a very clean reaction involving transfer of a methyl group from one metal center to the other,[10b] leading to $(CH_3)_2(PPh_3)Co(C_5H_4)CH_2(C_5H_4)Co(CO)_2$ (cf. Scheme II). These divergent results prompted us to investigate the reaction of PPh_3 with $[Cp^*Rh(CO)(CH_3)]_2$.

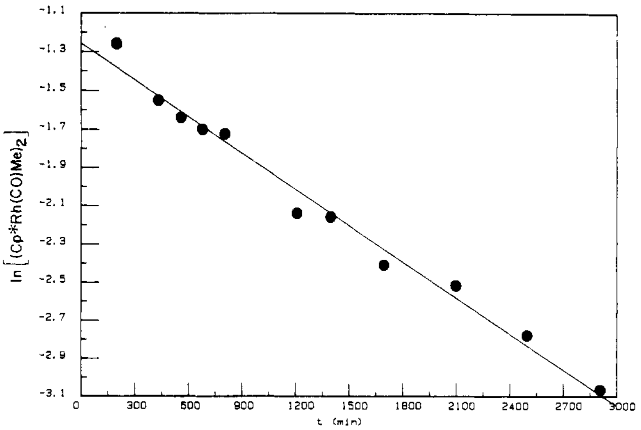

Figure 4. Sample kinetic plot for the disappearance of $[Cp^*Rh(CO)(CH_3)_2]$ vs. time in a run in which $[PPh_3]$ = 0.191 M.

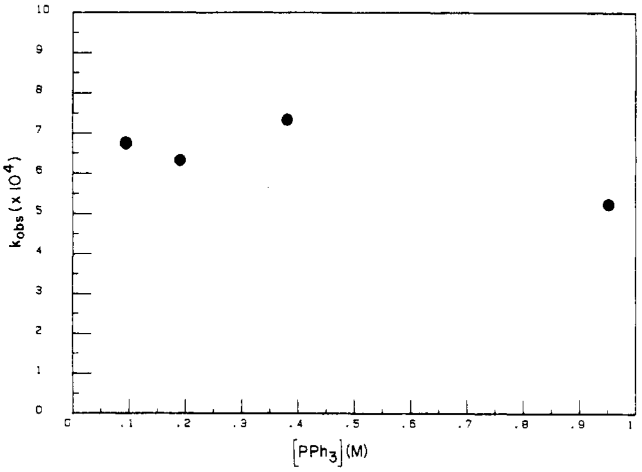

Figure 5. Dependence of k_{obsd} upon phosphine concentration for the reaction of $[Cp^*Rh(CO)(CH_3)_2]$ with PPh_3.

Scheme IV

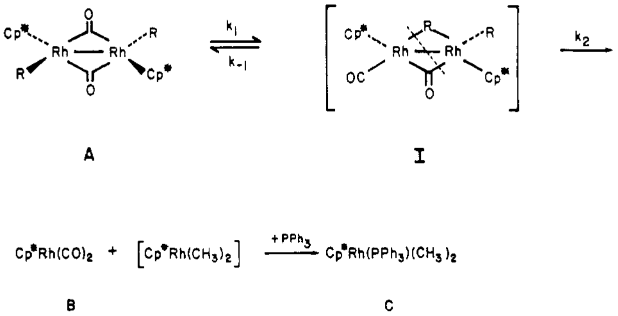

Treatment of the dinuclear dimethyl complex with PPh_3 gave a clean reaction analogous to that observed in the linked-ring cobalt system—i.e., equal amounts of $Cp^*Rh(PPh_3)(CH_3)_2$ and $Cp^*Rh(CO)_2$ were formed in high yield. Unlike the cobalt system, however, this reaction was effectively irreversible; it proceeded to completion without evidence for any reconversion of product to metal–metal-bonded starting material under the reaction conditions. This provided an opportunity to evaluate the kinetics of the reaction by using a less complicated analysis than that required in the cobalt system. In the presence of an excess

---

[40] Many attempts were made to synthesize $Cp^*Rh(CO)(CH_3)_2$. Attempts to make the carbonyl complex analogously to other $Cp^*Rh(L)(CH_3)_2$ compounds[41] by treating $[Cp^*RhCl_2]_2$ and $[Cp^*RhI_2]_2$ with CO and Me_3Al, MeLi, or MeMgBr or by reacting $Cp^*Rh(DMSO)(CH_3)_2$[41c] with CO at various temperatures led to isolation of either none or only trace amounts of the desired complex. One reaction did yield a small amount of spectroscopically pure material; details and characterization data are given in the Experimental Section.

[41] (a) Vazquez de Miguel, A.; Isobe, K.; Taylor, B. F.; Nutton, A.; Maitlis, P. M. *J. Chem. Soc., Chem. Commun.* **1982**, 758. (b) Isobe, K.; Vazquez de Miguel, A.; Bailey, P. M.; Okeya, S.; Maitlis, P. M. *J. Chem. Soc., Dalton Trans.* **1983**, 1441. (c) Vazquez de Miguel, A.; Gomez, M.; Isobe, K.; Taylor, B. F.; Mann, B. E.; Maitlis; P. M. *Organometallics* **1983**, *2*, 1724.

[42] Kang, J. W.; Maitlis, P. M. *J. Organomet. Chem.* **1971**, *26*, 393.

[43] Moseley, K.; Kang, J. W.; Maitlis, P. M. *J. Chem. Soc. A* **1970**, 2875.

[44] Werner, H.; Klingert, B. *J. Organomet. Chem.* **1981**, *218*, 395.

of PPh_3, clean pseudo-first-order kinetics were observed for the decomposition of the dinuclear dimethyl complex (a representative kinetic plot is reproduced in Figure 4). Varying the concentration of PPh_3 had *no* effect on the measured k_{obsd} (Figure 5). This establishes that the reaction proceeds by rate-determining formation of a reactive intermediate, which is trapped by PPh_3 more rapidly than it is reconverted to starting material.

We postulate the mechanism shown in Scheme IV, analogous to that suggested for the linked-ring cobalt complex,[10b] to account for the similar behavior of the Cp*-substituted rhodium system. We assume that the parent cobalt system also undergoes this reaction but that concurrent rapid dissociation to 17-electron radicals, which may also react rapidly with PPh_3, produces additional mononuclear substitution products. This mechanism would show no phosphine dependence, in accord with our observations. However, certain variations of this hypothesis cannot be rigorously ruled out on the basis of our data. One alternative, diagrammed in eq 6, is that the initially formed intermediate I reacts with L, leading directly to B and C. Steady-state analysis of this mechanism gives the rate law in eq 7, which predicts "saturation"

$$\underset{A}{[Cp^*Rh(CO)(CH_3)]_2} \underset{k_{-1}}{\overset{k_1}{\rightleftharpoons}} I \xrightarrow{k_2[L]} \text{Products} \tag{6}$$

$$\frac{-d[A]}{dt} = \frac{k_1k_2[L]}{k_{-1}+k_2[L]}[A] = k_{obs}[A] \tag{7}$$

behavior in [L]. We cannot rule out the possibility that in our system (even at low [L]), $k_2[L]$ is always much larger than k_{-1}, and we are not reaching values of [L] low enough to observe "falloff" in k_{obsd}. However, it seems unlikely to us that the simple R-unbridging step k_{-1} would be this slow. A more reasonable alternative mechanism postulates that the alkyl-bridging and fragmentation steps are concerted, and starting material A leads directly to B and $Cp^*Rh(CH_3)_2$; the latter complex is then trapped by PPh_3 more rapidly than it returns to A. This is the mechanism postulated earlier for the linked-ring cobalt system,[10b] where return to starting material is entropically much more favorable than it is for B and $Cp^*Rh(CH_3)_2$, and thus a dependence of k_{obsd} on [L] appears at higher [L].

Summary. The reaction of $[Cp^*RhCO]_2$ with Na/K gives stepwise the products of one- and two-electron reduction. The structure of the dipotassium salt of the two-electron reduction product has been determined by X-ray diffraction. Alkylation of the reduced species provides access to dirhodium dimetallacycles and dialkyl compounds, which are more stable than their cobalt analogues. However, a much more effective synthetic route has been developed which involves the addition of organolithium reagent across the metal–metal multiple bond in $[Cp^*Rh(CO)]_2$, followed by treatment with electrophilic alkylating agents. This route is more versatile than that available in the corresponding cobalt system, in that it gives higher overall yields, is capable of producing mixed dialkyl complexes, and proceeds stereoselectively to give cis dialkyl complexes as kinetic products. The fact that cis/trans isomerization occurs rather slowly and, without mixing of alkyl groups, demonstrates that dissociation of the dinuclear complex into 17-electron monomers occurs much more slowly than in the corresponding cobalt complexes. Ligand-induced metal-to-metal alkyl transfer is still a facile and kinetically clean process, however, indicating that 17-electron monomers are not essential intermediates in this reaction. Further studies will be required to determine conclusively whether the alkyl transfer processes are truly dinuclear in nature.

Acknowledgment. We are grateful for financial support from the National Science Foundation (Grant No. CHE-8420979), the X-ray crystal structure analysis performed by Dr. F. J. Hollander of the UC Berkeley X-ray diffraction facility (CHEXRAY), and assistance with the electrochemistry experiments by Professor Marcin Majda and Mr. Cary Miller. We also acknowledge a generous loan of rhodium chloride from Johnson-Matthey, Inc., as well as assistance with the ESR experiments by Dr. Melvin Klein and Dr. Paul Seidler and magnetic susceptibility measurements performed by Mr. Dave Berg.

Registry No. $K^+[Cp^*RhCO]_2^-$, 96040-99-2; $[Cp^*RhCO]_2$, 69728-34-3; $[K(Crypt)^+][Cp^*RhCO]_2^-$, 96055-52-6; $(K^+)_2[Cp^*RhCO]_2$, 96041-01-9; $[K(Crypt)^+]_2[Cp^*RhCO]_2^{2-}$, 96041-03-1; $[Cp^*RhCO]_2(\mu\text{-}CH_2)$, 76550-26-0; $[Cp^*Rh(CO)]_2(CH_2)_3$, 96041-04-2; *cis*-$[Cp^*Rh(CO)(CH_3)]_2$, 96041-05-3; $[Cp^*{}_2Rh_2(CO)_2(CH_3)]$, 103731-60-8; $[Cp^*{}_2Rh_2(CO)_2(C_2H_5)]$, 96055-54-8; $[Cp^*{}_2Rh_2(CO)_2(C_6H_5)]$, 103731-61-9; *cis*-$[Cp^*{}_2Rh_2(CO)_2(CH_3)(CD_3)]$, 103731-62-0; *cis*-$[Cp^*{}_2Rh_2(CO)_2(CH_3)(C_2H_5)]$, 96148-94-6; *cis*-$[Cp^*Rh(CO)(C_2H_5)]_2$, 96041-07-5; *cis*-$[Cp^*{}_2Rh_2(CO)_2(C_6H_5)(CH_3)]$, 103731-63-1; $Cp^*Rh(CO)(CH_3)_2$, 103731-64-2; $[Cp^*RhCl_2]_2$, 12354-85-7; $(K^+)_2[Cp^*RhCO]_2^{2-}\cdot 2THF$, 96041-08-6; $Cp^*Rh(C_2H_4)_2$, 32613-78-8; $Cp^*Rh(CO)[P(CH_3)_3]$, 80182-11-2; $Cp^*Rh[P(CH_3)_3](CH_3)_2$, 103731-65-3; $(TsO)(CH_2)_3(OTs)$, 5469-66-9; C_2H_4, 74-85-1.